Universidade de Lisboa
Faculdade de Ciências
Departamento de Química e Bioquímica

Broad-spectrum antiviral peptides against respiratory viruses

Patrícia Morgado da Silva

Mestrado em Bioquímica

Especialização em Bioquímica Médica

Dissertação orientada por:
Prof. Doutor Nuno C. Santos e Prof. Doutor Francisco Pinto

2016

Acknowledgments

Firstly, I would like to express my sincere gratitude to Prof. Nuno C. Santos, my supervisor, for all the availability and mainly for the opportunity to join his research group in order to develop my master thesis. In the Biomembranes Unit I had the opportunity to have contact with people that have developed Science for so long and they were a giant help in my scientific education. In the beginning of this "adventure", one person had the patience to help me understand all the work that were already made in this Unit, explained to me all the techniques and gave me the know-how to complete this Thesis, therefore, thank you Marcelo Augusto.

I would like to thank Marta Marques for all the never-ending patience, support and friendship that she gave me for all this year.

To everyone of the Biomembranes Unit I would like to express my gratitude for making me feel like home, especially to Catarina Lopes, Patrícia Carvalho, Filomena Carvalho and Teresa Freitas. You are the best!

I also would like to thank all my friends for their support and encouragement. Gonçalo Santos, Patrícia Cortimpau, Margarida Besouro, Joana Fernandes, Neuza Catarina, Marisa Maia, I am so lucky to be able to call you friends!

A big thank for Ana Rodrigues and Filipe Rodrigues for never stop believing in me, you were a major help!

I wish to thank my parents and my brother for giving me the opportunity and all the conditions to continue my studies, I know that it was not easy and for that I am eternally grateful!

And, last but not the least, I would like to thank a very special person to me, Bruno Rodrigues. Thank you for all the love, care, support and patience, not only for this year, but for the almost six years that I have been given the privilege to be at your side. You always believed in me, even when I didn't. Thank you for everything!

Resumo

O vírus Influenza A pertence à família *Orthomyxoviridae* sendo responsável por transmitir infeções virais agudas do trato respiratório, como a gripe. Este vírus apresenta uma distribuição a nível global e uma elevada taxa de transmissibilidade. A gripe afeta maioritariamente crianças, idosos e pessoas com o sistema imunitário mais debilitado. Apresenta como sintomas, febre, dores de garganta, dores musculares, dores de cabeça, tosse, fadiga e sensação geral de desconforto.

Este vírus normalmente é transmitido por via aérea através de tosse ou de espirros, isto porque através destas ações são libertadas partículas que contêm o vírus. Estas partículas podem ser inaladas por outras pessoas, infetando as mesmas, acabando por desencadear a doença. Outra forma de transmitir a gripe é através do contacto com superfícies contaminadas.

O vírus influenza A apresenta uma forma esférica e contém um envelope viral onde estão inseridas duas glicoproteínas, a hemaglutinina e a neuraminidase, e um canal iónico, o M2. O genoma viral é composto por RNA de cadeia simples negativa. A hemaglutinina apresenta um papel crucial na entrada do vírus para a célula, uma vez que é através da mesma que os recetores de acido siálico são reconhecidos e, para além disto, também participa no processo de fusão, onde após a diminuição do pH dentro do endossoma sofre uma alteração na sua conformação que a leva a expor o péptido de fusão. Por outro lado, a neuraminidase participa na libertação do vírus a partir das células infetadas.

A prevenção e o controlo da transmissão deste vírus passa pelas vacinas e antivirais já existentes no mercado. Devido à elevada taxa de mutação do genoma do vírus, o tratamento existente no mercado não é eficaz contra os vírus resistentes. É o caso dos inibidores da neuraminidase, como o oseltamivir e zanamivir, e os inibidores do canal iónico M2, como a amantidina e rimantadina, que impedem que o vírus infete células. Estes antivirais já são comercializados, no entanto, têm vindo a ser retirados do mercado devido à existência de efeitos secundários graves e pelo facto de os vírus que têm aparecido mais recentemente apresentarem mutações resistentes a estes antivirais. Deste modo, é importante encontrar novos alvos de ação para combater a infeção por parte do vírus

influenza. Uma das hipóteses passa por desenvolver agentes antivirais, que têm a capacidade de inibir a fusão membranar entre o vírus e a célula-alvo. Esta estratégia foi aplicada com sucesso contra o vírus da imunodeficiência humana (HIV), estando a ser alargada para mais vírus envelopados como é o caso do vírus influenza.

A inibição da fusão das membranas virais e do hospedeiro é uma estratégia que tem vindo a ser estudada. Este passo é essencial para a infeção da célula alvo por parte do vírus. Uma vez inibido, o vírus perde a capacidade de infectar a célula do hospedeiro, e como consequência não ocorre a propagação viral dentro do hospedeiro.

Nesta dissertação foram estudados três péptidos com potencial para inibir a fusão membranar do vírus influenza com a membrana celular. Estes péptidos foram desenhados a partir da região CHR da cadeia HA_2 da hemaglutinina, que aparenta ser a zona mais conservada da proteína. Todos os péptidos derivados dessa região têm a denominação de péptidos C ou inibidores de fusão classe I. Portanto, estes péptidos mimetizam a região CHR da proteína viral hemaglutinina e ligam-se à região complementar (NHR) também pertencente à mesma proteína.

Os três péptidos em estudo apresentam a mesma sequência peptídica, contundo são diferentes entre si em temos de derivatização. A denominação “Influenza” será atribuída à sequência peptídica. O primeiro péptido, Influenza-PEG_4-Colesterol, apresenta um espaçador com quatro unidades de polietilenoglicol que separa a região peptídica e um domínio lípido, o colesterol. Este péptido já foi estudado anteriormente por nossos colaboradores do Centro Médico da Universidade de Columbia, em Nova Iorque, que tambem nos forneceram estes péptidos. Pelos estudos realizados com o péptido foi possível concluir que este consegue bloquear a fusão do vírus através da ligação à hemaglutinina e posteriormente incapacitando a mesma de alterar a sua conformação, que é um passo essencial para a fusão. Os restantes dois péptidos são derivados do Influenza-PEG_4-Colesterol, sendo que um apresenta apenas a cadeia peptídica sem domínio lipídico e o outro é constituído por duas cadeias peptídicas e está conjugado com uma molécula de colesterol, (Influenza-PEG_4)$_2$-Colesterol. Este projeto teve como objetivo estudar a interação do péptido Influenza-PEG_4-Colesterol e os seus derivados com sistemas modelo de biomembranas e igualmente com membranas de algumas células do sangue, nomeadamente eritrócitos e linfócitos.

A avaliação desta interação foi efetuada através de metodologias de espectroscopia de fluorescência. O primeiro ensaio teve como objetivo avaliar se os péptidos interagem com a membrana de vesiculas lipídicas de diferentes composições, POPC e de POPC:Colesterol (2:1). Esta avaliação é possível uma vez que os péptidos apresentam um ou dois (no caso do dímero) resíduos de triptofano na sua constituição e como se sabe, o triptofano apresenta fluorescência intrínseca. Esta fluorescência intrínseca é uma ferramenta válida para averiguar a inserção dos péptidos nas vesiculas, sendo que à medida que existe uma alteração da fluorescência é sinal que o péptido estará mais inserido na membrana. Neste caso, através da excitação seletiva dos resíduos de triptofano e deteção da emissão de fluorescência dos mesmos, foi possível observar que o dímero apresentou maioritariamente melhores resultados, tendo tido valores de K_p superiores aos dos restantes péptidos, tendo maior afinidade para vesículas que contêm colesterol.

Uma vez que estes péptidos apresentam colesterol na sua constituição, têm uma maior tendência para formar agregados. Através da sonda ANS que se torna fluorescente quando se insere em microambientes hidrófobos, foi possível observar que tanto o Influenza-PEG_4-Colesterol como o (Influenza-PEG_4)$_2$-Colesterol agregam em solução. Como já era expectável, o péptido que não apresenta nenhuma componente lipídica, não sofre agregação.

De seguida, através de extintores de fluorescência em solução aquosa (acrilamida) e em membrana (5NS e 16NS) foi possível determinar a posição do resíduo de triptofano nas membranas lipídicas. O péptido que não apresenta nenhum domínio lipídico, apresenta o resíduo de triptofano bastante acessível ao ambiente aquoso, o que nos permite explicar a não existência de partição das membranas. Os restantes péptidos mostraram estar mais inseridos na membrana e por isso, sofreram menos extinção de fluorescência por parte da acrilamida.

A presença do domínio lipídico poderá permitir ao péptido uma maior interação com as membranas. De maneira a avaliar esta interação foi utilizada uma sonda sensível ao potencial de dipolo das membranas, a sonda di-8-ANEPPS. Inicialmente foram marcados lipossomas com esta sonda para testar a interação dos péptidos com os mesmos. Neste caso, não foi registada praticamente nenhuma alteração no potencial de dipolo das membranas dos lipossomas. De maneira a estudar a interação com células, tanto os

eritrócitos como os linfócitos foram marcadas com a mesma sonda. Contrariamente ao que foi observado com os lipossomas, já houve uma maior interação por parte dos péptidos com as membranas das células. O Influenza-PEG_4-Colesterol demonstrou ter maior afinidade para os eritrócitos a pH 7 e o péptido (Influenza-PEG_4)$_2$-Colesterol demonstrou ter uma afinidade maior para os linfócitos, também a pH 7. Um estudo realizado neste grupo, para péptidos inibidores de fusão para o HIV, o HIVP4 (que é também um dímero com um domínio de colesterol) também apresentou uma maior afinidade para linfócitos.

Resumidamente, o péptido que não tem colesterol não interage com as membranas lipídicas através do resíduo de triptofano, nem aparenta agregar em solução aquosa devido a ausência de domínio de colesterol. Em relação ao dímero, este apresentou melhores resultados na partição e na interação com células. Este péptido foi o que apresentou uma melhor afinidade quando presente em ambiente com pH acídico. O facto de este péptido apresentar melhores resultados que o monómero poderá demonstrar que a dimerização do péptido pode ser fundamental, uma vez que influencia a concentração do péptido ao nível da membrana.

A conjugação de um domínio lipídico, como o colesterol, e a dimerização aparentam ser estratégias que aumentam a atividade antiviral dos possíveis inibidores de fusão do influenza A.

Abstract

Influenza viruses (IV) are major human pathogens responsible for respiratory diseases affecting millions of people worldwide and characterized by high morbidity and mortality. Infections by influenza can be controlled by vaccines and antiviral drugs. However, this virus is constantly under mutations, leading to growing resistance to influenza antivirals currently in use. It is urgent to develop new strategies for therapeutics. Influenza hemagglutinin (HA) is a potential target for antiviral drugs, because it is a key protein in the initial stages of infection. This protein is involved in receptor binding and promotes the (pH-dependent) fusion of virus and cell membranes after endocytosis. HA-targeted peptides are expected to lead to novel anti-influenza drugs. Cholesterol conjugated HA-derived peptides with anti-fusion activity against influenza have been previously studied on live virus. In this study, we evaluated three HA-derived peptides using fluorescence spectroscopy. Membrane partition assays were performed at two different pH values to assess the interaction with biomembrane model systems and (Influenza-PEG_4)$_2$-Chol presented the highest partition in all the conditions. Peptide aggregation was also assessed by the ANS probe. Human blood cells were used to evaluate the extent of cell membrane binding, using the dipole potential probe di-8-ANEPPS. In this assay the dimer peptide showed to have higher affinity for PBMC and the monomer for erythrocytes. Preferential localization of tryptophan in lipid bilayers was also assessed, using aqueous-soluble and lipophilic quenchers. It was possible to observe that the untagged peptide is at a shallow position. Therefore, the tryptophan residue is more accessible to acrylamide and the cholesterol-tagged peptides are more inserted in the membranes. In conclusion, cholesterol-tagged peptides and dimerization may be used to increase the activity of the peptides. Our results provide new insight into molecular interactions between HA-derived peptides and cell membranes, which may contribute toward the development of new influenza A virus inhibitors.

Key words: Influenza A, viral fusion inhibitors, peptides, cholesterol-tagging, dimerization

Contents

List of figures and tables

Symbols and Abbreviations

16NS – 16-doxyl-stearic acid

5NS - 5-doxyl-stearic acid

Chol – Cholesterol

CHR – C-terminal heptad repeat domain

Di-8-ANEPPS – 4-[2-[6-(dioctylamino)-2-naphthalenyl] ethenyl]-1-(3-sulfopropyl)-pyridinium)

DMSO – Dimethylsulfoxide

ER – Endoplasmatic reticulum

f_B – Fraction of fluorophores accessible to the quencher

Flu – Influenza

FP – Fusion peptide

HA – Hemagglutinin

HEPES – 4-(2-hydroxyethyl)-1-piperazineethanesulfonic acid

HR – Heptad repeat regions

IAV – Influenza A virus

IMM- Instituto de Medicina Molecular

IPS – Instituto Português do Sangue

IV – Influenza Viruses

K_p – Partition coefficient

K_{sv} – Stern-Volmer constant

LBD – Lipid binding domain

LUV – Large unilamellar vesicles

MLV – Multilamellar vesicle

NA – Neuraminidase

NEP – Nuclear Export Protein

NHR – N-terminal heptad repeat domain

n_L – Number of moles of lipid

$n_{peptide,\ L}$ – Number of moles of peptide present in the lipid phase

$n_{peptide, W}$ – Number of moles of peptide present in the aqueous phase

n_W – Number of moles of water

PBD – Pocket binding domain

PBMC – Peripheral blood mononuclear cell

POPC – 1-palmitoyl-2-oleoyl-sn-glycero-3-phosphocoline

RBC - Red blood cells; erythrocytes

RBP – Receptor binding pocket

RNP – Ribonucleoprotein

TM – Transmembrane domain

vRNP - Viral Ribonucleoprotein

$\Delta\psi$ - Transmembrane potencial

λ_{ex} – Excitation wavelength

ψ_d – Dipole potencial

ψ_s - Surface potencial

1. Introduction

1.1 Influenza viruses

Influenza viruses (IV) are major human pathogens responsible for respiratory diseases affecting millions of people worldwide and characterized by high morbidity and significant mortality (Loregian et al. 2014). The high mortality results not only from pneumonia and influenza, but also from cardiopulmonary and other chronic diseases that can be exacerbated by the virus.

IV belong to the *Orthomyxoviridae* family and is classified into three types, A, B and C (Hamilton et al. 2012). The three types of influenza viruses differ in host range and pathogenicity. Influenza A is the most dangerous, since it infects a large number of warm-blooded animals (Taubenberger & Morens 2010), being also found in blood circulation more often (Figure 1), while influenza B viruses infect almost exclusively humans (Loregian et al. 2014). These two types of influenza viruses are responsible for significant morbidity and mortality in infants and elderly people (Vanderlinden & Naesens 2014).

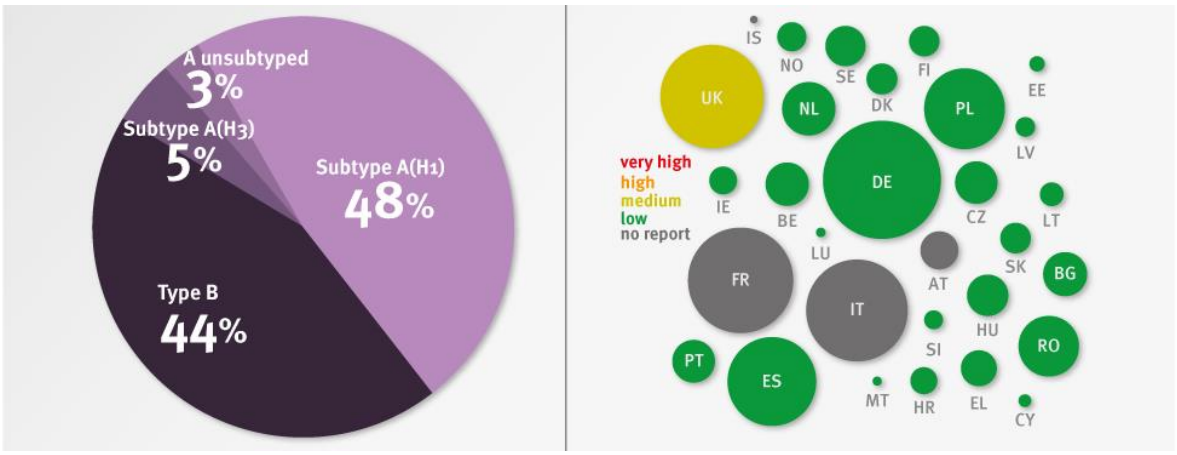

Figure 1: Influenza viruses circulating in 2015/2016 and influenza intensity in May 2016, in Europe.
Bubbles correspond to different countries and the bubble size is indicative of country population.
Source: Adapted from European Centre for Disease Prevention and Control

Influenza virus A (IAV) is considered a serious threat to public health. It causes a high impact at the socioeconomic level, due to the seasonal influenza epidemics and influenza pandemics. Seasonal flu epidemics normally occur mainly in the winter in temperate climes (Taubenberger & Morens 2010) and it is responsible for about 50000 deaths per year (Yang et al. 2013). However, pandemics can be more deadly than seasonal flu epidemics.

Pandemics occur when the avian influenza A crosses the specie barrier into humans and the spread occurs efficiently from human to human (Yang et al. 2013).

All over the years, pandemics have been demonstrating their impact in world. The "Spanish" influenza pandemics that occurred in 1918 still stands as the single most fatal event in human history, known for causing the death to 50 million of people (Taubenberger 2006). The causative agent was an avian-descended H1N1 virus (Taubenberger & Morens 2010). The most recent pandemic occurred in 2009 and it was considered the first influenza pandemic of the twenty-first century. It started in Mexico in mid-February. In May the virus was already spread into 41 countries and killed 85 persons (Neumann et al. 2009).

Due to its historical events (Figure 2), influenza A is one of the greatest threats to humankind, being compared to other viruses with major impact in human health such as HIV and Ebola. These viruses present a higher mortality if untreated, but they lack influenza inter-personal transmission or its widespread seasonal distribution, respectively. In a year of new pandemic, Influenza has 4 times the total mortality attributed to HIV in the last 30 years (Gatherer 2009).

Figure 2: Timeline of Human Flu Pandemics
Where ■ correspond to major pandemic and ● correspond to the appearance of a new influenza strain in the human population. Source: National Institute of Allergy and Infectious Disease.

Now it is clear that the influenza pandemics occur at unpredictable intervals. However, there are emerging threats of novel pandemic influenza strains spreading in the human population. To deal with it, research efforts have been encouraged in order to develop new therapies against influenza viruses.

1.2 Virus structure and replication cycle

1.2.1 Structure

The influenza virion is roughly spherical. It is enveloped by a lipid membrane contains two glycoproteins – hemagglutinin (HA) and neuraminidase (NA) - and also a small integral membrane protein, M2 (Figure 3) (Bouvier & Palese 2008). Influenza A virus comprises 18 hemagglutinin (Edinger et al. 2014) and 9 neuraminidase subtypes, determined by the distinct antigenicity of each of these protein (Medina & García-Sastre 2011).

Beneath the lipid membrane there is a viral protein named M1, or matrix protein. This protein, which forms a shell, gives strength and rigidity to the lipid envelope. Within the interior of the virion, one may find the nuclear export protein (NEP) and the ribonucleoprotein (RNP) complex, which consists of the viral RNA segments coated with nucleoprotein (NP) and the heterotrimeric RNA-dependent RNA polymerase (PB1, PB2 and PA) (Bouvier & Palese 2008). The single-stranded, negative-oriented RNA genome is divided over eight viral ribonucleoprotein (vRNP) segments (Vanderlinden & Naesens 2014).

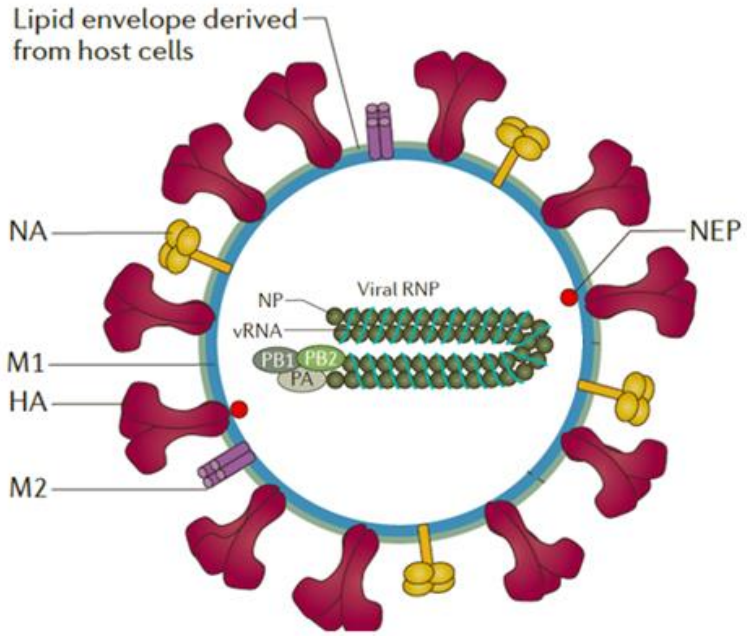

Figure 3: Influenza virus structure
Adapted from (Medina & García-Sastre 2011)

1.2.2 Replication cycle

The entry process of the virus represents a potential target for drug development. Influenza A virus entry is a dynamic process that requires the achievement of six individual steps: binding to target cells, internalization into cellular compartments, endosomal trafficking, fusion of viral and endosomal membranes, uncoating and importing of the viral genome into the nucleus.

The first step is initiated by the recognition and binding of the receptor sialic acid (N-acetylneuramic acid) by hemagglutinin (Edinger et al. 2014). After binding, the virus is internalized by endocytosis. Influenza A virus is capable of using multiple endocytosis routes, which is clear because it was already observed that IAV could internalize mainly into clathrin-coated but also uncoated vesicles (Sieczkarski & Whittaker 2002). During maturation of the endosome, the pH drops from 7 to around 5, leading to a consequent conformational change in HA that initializes the fusion of the viral envelope with the endosomal membrane. The conformational changes that occur in HA are necessary to expose the fusion peptide (Vanderlinden and Naesens 2014) . Afterwards, it is inserted into the target membrane, bringing the viral and endosomal membranes into close proximity, leading to the creation of the fusion pore (Hamilton et al. 2012) . After the fusion, occurs the release of the viral RNA and viral proteins into the cytosol, through the fusion pore. This process is called uncoating and requires coordinated action of the M2 and M1 proteins, where M2 is responsible for the pH drops in the endosome by the mediation of proton influx. M2-mediated change in pH is required for the detachment of M1 from the viral RNA, resulting in its release to the cytosol (Edinger et al. 2014). The viral RNA traffics to the nucleus, where the viral polymerase starts mRNA synthesis and therefore its mRNA transcription is initiated. Newly formed viral RNAs are exported to the cytosol, where they assemble with new virus structural proteins, which are processed in the endoplasmic reticulum (ER) and the Golgi apparatus and subsequently transported to the cell membrane. As the vRNPs reach the cell membrane, they associate with viral glycoproteins at the plasma membrane from which new virions bud off. At last, NA cleaves the sialic acid termini on viral and cell membrane glycoproteins achieving the release of new virions from the host cell (Figure 4) (Das et al. 2010).

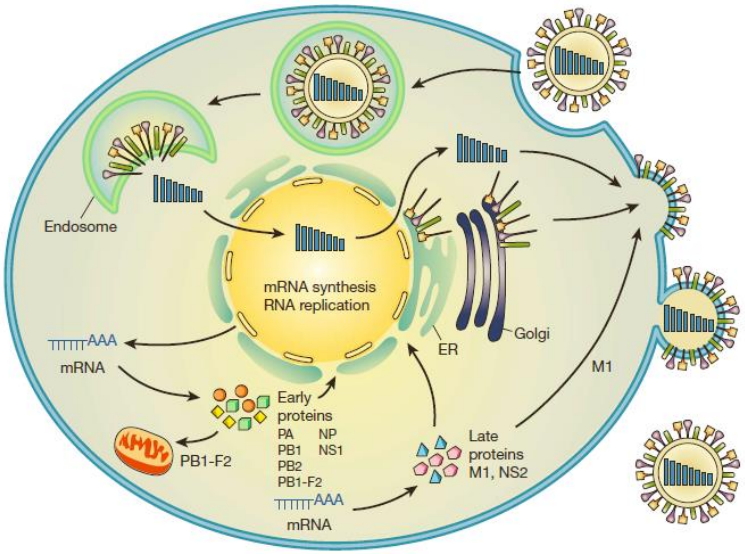

Figure 4: Schematic diagram of the influenza viral life cycle.
(Neumann et al. 2009)

1.3 Transmission of influenza virus

Transmission of an infectious disease is the process by which an infectious organism moves from one host to another and causes disease (Killingley & Nguyen-Van-Tam 2013). Limited understanding of influenza transmission has been a frequent obstacle during the development of pandemic influenza infection prevention.

The entry and exit of the virus in humans occur through the respiratory tract, that is, mouth and nose. Viruses are released from an infected host during events such as coughing, sneezing and talking. After these events, the virus is able to entry in a new host via inhalation or direct and indirect contact (Killingley & Nguyen-Van-Tam 2013).

There are a huge number of factors that may contribute to an effective or a non-effective transmission of the influenza virus, as we can see in figure 5.

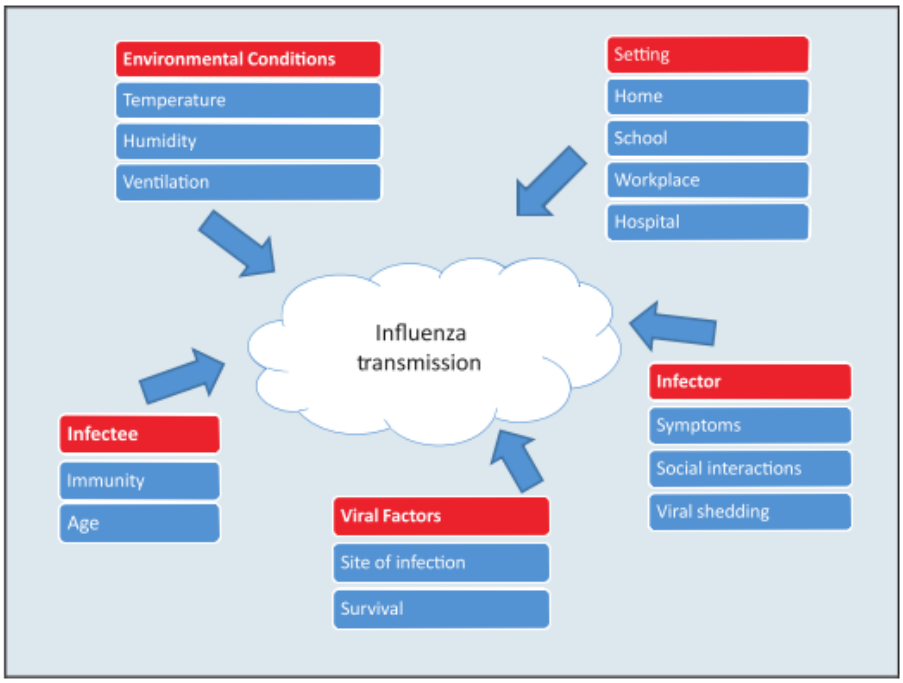

Figure 5: Factors that affect influenza transmission.
(Killingley & Nguyen-Van-Tam 2013)

However, three routes of influenza transmission are widely accepted, namely:

- Aerosols: these particles are small enough to be inhaled (<5 μm) and reach the lower respiratory tract (Cowling et al. 2013).
- Droplets: these particles can deposit on mucous surfaces of the upper respiratory tract such as the mouth and nose. They can be inhaled but are too large (>10 μm) to reach the lungs (Willem et al. 2012).
- Contact transmission: particles are transferred to mucous membranes of the upper respiratory tract either directly or indirectly, via a contaminated object or person, (Herfst et al. 2012).

Moreover, in order for the viruses to cause an infection, they must survive in the environment and reach the target cells in a host and finally, enough virus must reach its target cells to achieve an infectious dose to initiate the infection (Killingley & Nguyen-Van-Tam 2013).

Understanding how and why the viruses spread so efficiently among people and determining possible ways to harness this transmission have been arduous tasks, given the limitations of flu animal models (Lakdawala & Subbarao 2012). This knowledge is crucial to the development of new and effective ways to prevent the transmission of this virus.

1.4 Prevention and control

Influenza infections can be controlled by vaccination and antiviral drugs (Neumann et al. 2009; Loregian et al. 2014).

Vaccines give limited protection and need annual updating, due to antigenic drift. Antigenic drift is a mechanism for variation in viruses that involves the accumulation of mutations (Krammer & Palese 2015). This results in a new strain of virus particles, which cannot be inhibited as effectively by the antibodies, as they were originally targeted against previous strains, making it easier for the mutant virus to spread throughout a partially immune population.

There are two major problems relating to pandemic influenza vaccines: the time between virus identification and vaccine development and distribution (Figure 6), and the weak immune responses (low immunogenicity) (Krammer & Palese 2015).

Rapid vaccine production is vital for reducing global morbidity and mortality. The production of a vaccine against a newly emerging strain would take about 7 – 8 months, enough time for a virus to spread globally and substantially strain health care systems and global economy.

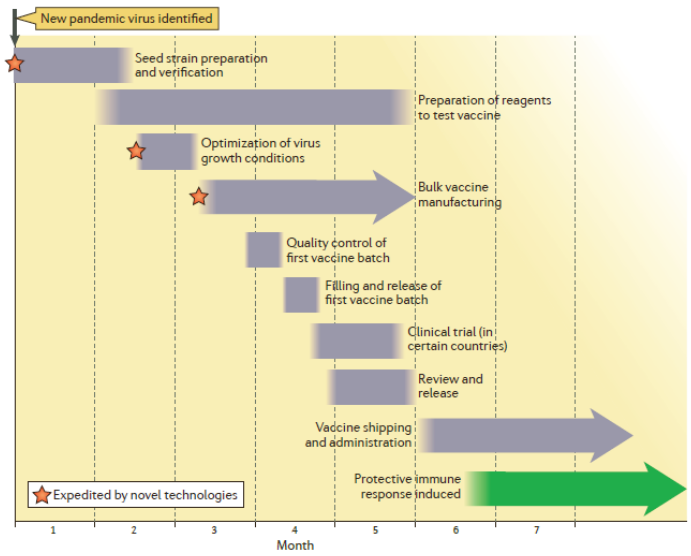

Figure 6: Influenza virus vaccine production process.
(Krammer & Palese 2015)

At present, influenza is the only respiratory virus against which antiviral drugs are commercially available (Heikkinen 2016). The available drugs include the neuraminidase (NA) inhibitors oseltamivir (oral administration) and zanamivir (administration by inhalation); and, M2 ion channel blockers, such as amantadine and rimantadine (Skalickova et al. 2015). For young children, oseltamivir is the only option (Heikkinen 2016).

Although ion channel inhibitors can be effective against influenza virus infection, they have been reported to cause central nervous system side effects. Also, the currently circulating influenza strains are resistant to these antivirals that block the ion channel formed by M2. In case of the neuraminidase inhibitors, they interfere with NA enzyme activity, which is critical for the release of newly synthesized virus from infected cells (Yang et al. 2013). However, the currently available drugs suffer from rapid and extensive emergence of drug resistance, due to the resistant viruses that are constantly emerging.

Several new classes of antiviral agents targeting viral replication mechanisms or cellular proteins/processes are under development (Loregian et al. 2014).

All of this highlights the urgent need for developing new antiviral strategies with novel mechanisms of action and with reduced drug resistance potential.

1.5 Hemagglutinin (HA)

Hemagglutinin is the viral protein that mediates the entry of influenza viruses into host cells. This protein controls two critical aspects of entry: virus binding and membrane fusion (Hamilton et al. 2012).

In virion surface, HA is expressed as a trimer. The stalk region of HA connects it to the virion envelope by a short hydrophobic sequence (Skehel & Wiley 2000). The stability and the structure of this protein are afforded by the fact that the stalk region is heavily glycosylated on conserved epitopes (Roberts et al. 1993).

The HA protein contains multiple disulfide bonds and is cleaved into a mature form consisting of two subunits, HA1 and HA2. The receptor binding pocket (RBP) is located on the distal end of the HA trimers, at the globular head, and is highly conserved among different HA subtypes (Figure 7). The receptor sialic acid is the major point of contact between the virus and the cell and occupies the whole RBP. The interaction between the receptor and the protein is known to be of low affinity. In order to increase it, multiple HA molecules are used to bind several glycoproteins (Edinger et al. 2014).

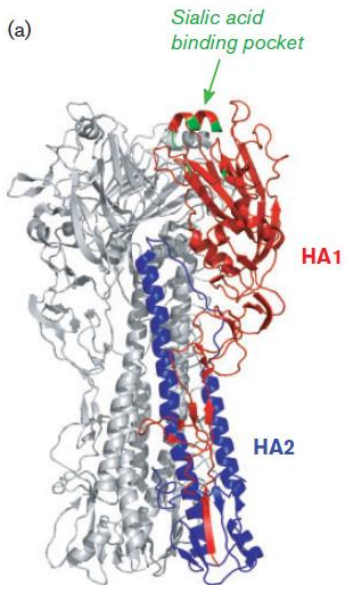

Figure 7: Structure of the HA
The trimeric complex is shown with one monomer highlighted in color. Adapted from (Edinger et al. 2014)

As previously mentioned, at acid pH, the membrane fusion potential of HA is activated in endosomes by the induction of an irreversible reorganization of its structure. In figure 8, we can see the major change on HA conformation: a dissociation of HA_1 from the endosomal membrane and its movement away from HA_2, a loop-to-α-helix transition in HA_2 enables the fusion peptide at the N terminus of HA_2 to attach to the endosomal membrane and promote the fusion of the viral and endosomal membranes, resulting in the release of the viral RNA into the cytoplasm (Russell et al. 2008). Small molecules that block this irreversible reorganization of HA would be expected to inhibit virus entry.

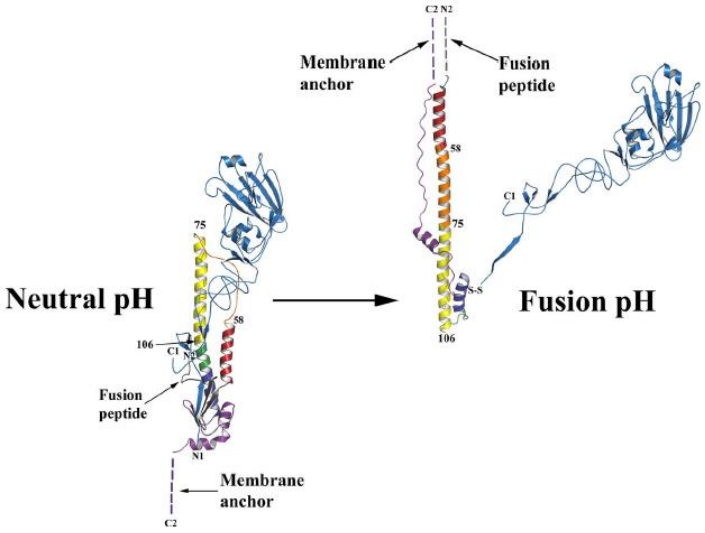

Figure 8: Structure of HA at neutral pH and at fusion pH
The disulfide-linked polypeptide chains, HA_1 and HA_2 are colored blue and multicolored, respectively. (Russell et al. 2008)

The hemagglutinin is also known to bind to sialic acid receptor on the surface of red blood cells (RBC) and create a network of interconnected RBC's and virus particles; this process is called hemagglutination (Figure 9). The formation of this network depends on the concentrations of the virus and RBC's. This process is used as a method for quantification the relative concentration of the virus in the host (Mammen et al. 1995; Fox et al. 2015).

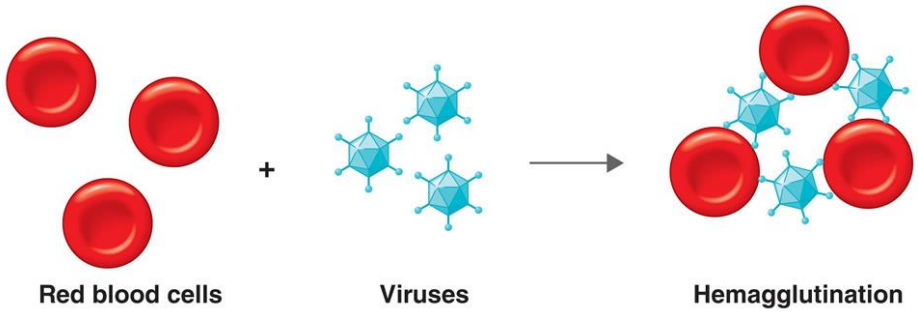

Figure 9: Viral Hemagglutination
Source: Practical Applications of Immunology

1.6 Antiviral Peptides against viral fusion

Membrane fusion for viral entry is a key step in viral infectivity, therefore, interference with this process can lead to highly effective antivirals. Fusion is driven by specialized proteins that undergo a series of conformational changes. They can be classified according to three classes of viral fusogenic membrane glycoprotein based on their mechanism of fusion and structure organization (Figure 10):

- Class I fusion proteins: Comprises Influenza A, paramyxovirus F, HIV and Ebola virus. All the proteins from this class form homotrimers. Initially, they are synthesized as fusion-inactive precursor molecules and, depending on the viral family, can be activated in order to expose the N-terminus of the fusion peptide by three ways. The first one is by acidic pH, which is the influenza HA case; the second one is by direct receptor binding and conjugation with acidic pH and at least, the activation also can occur by the receptor binding by a non-covalently associated envelope glycoprotein that stimulates refolding of the fusion protein in neutral pH (Plemper 2011). Class I proteins have two heptad repeat (HR) domains, one adjacent to the fusion peptide, the N-terminal heptad repeat domain (HRN), and other immediately preceding the transmembrane domain, the C-terminal heptad repeat domain (CHR) (Porotto et al. 2010). The NHR and CHR refolding create the stable six-helical bundle (6HB) structure. 6HB formation is linked to the creation of the fusion pore and it is known that this structure stimulate the pore formation and expansion (Plemper 2011).

- Class II fusion proteins: Dengue is a virus that contains this type of protein. It is the only class that shows a dimeric prefusion conformation, forming an elongated structure parallel to the viral envelope. This fusion is triggered by low pH, extending the fusion loops towards the target membrane. The final protein structure remains rich in β-sheets (Plemper 2011).

- Class III fusion proteins: Comprises rhabdovirus and herpesvirus. The protein is a trimer in both pre- and postfusion conformations. This fusion is triggered by low pH, inducing swinging of the tripod legs towards the target membrane and the postfusion structures resembles six-helix bundles of class I proteins, but lacks heptad repeated domains (Plemper 2011).

These three classes of fusion proteins act as functional trimers when driving the membrane fusion process and they all fold into stable trimers in the postfusion conformation.

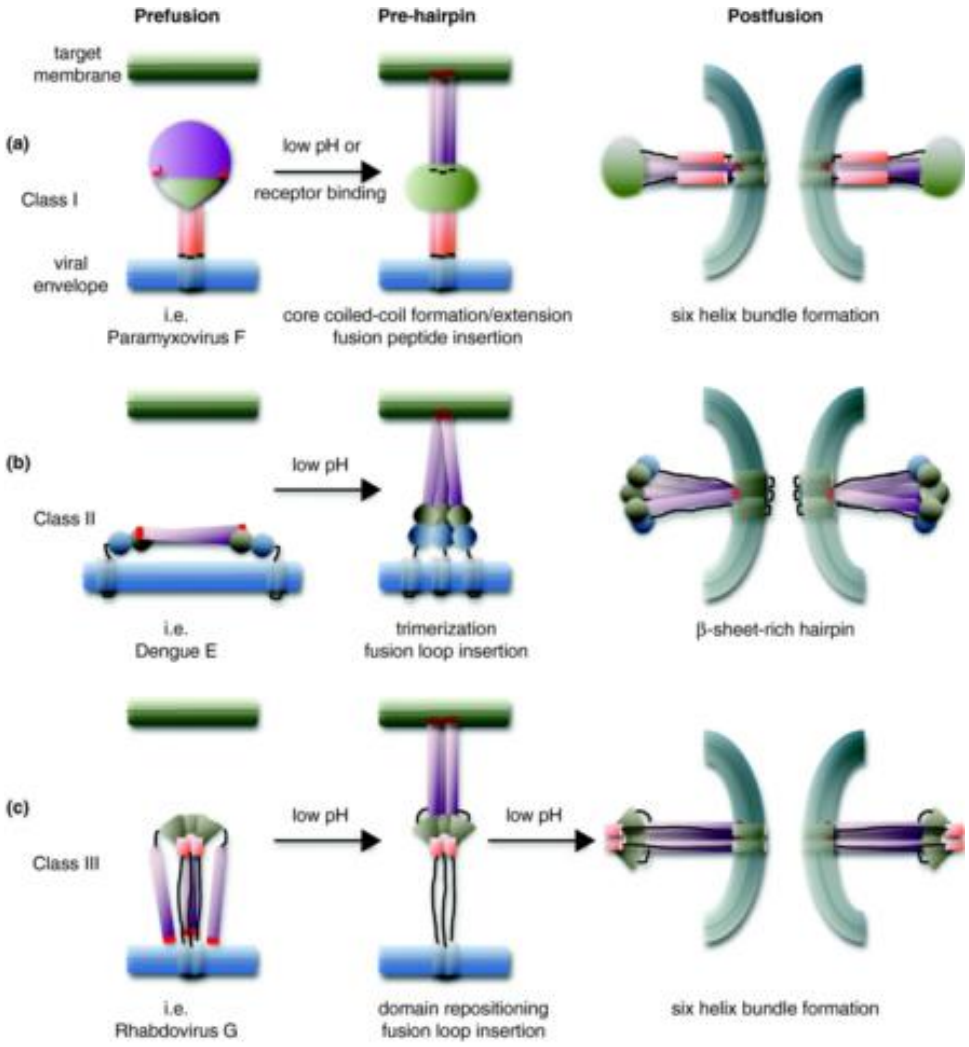

Figure 10: Schematic representation of the general domain organization and conformational reorganization of the three viral fusion protein classes.
(Plemper 2011)

Understanding the different conformational changes that take place in the three classes of fusion proteins is necessary to design fusion inhibitor peptides that can prevent those changes during the infection process (Vigant et al. 2015). Therefore, peptides derived from the HR regions, are known to inhibit fusion. These peptides bind to their complementary HR region and prevent NHR and CHR from refolding into the stable six-helical bundle (6HB) structure required for fusion initiation (Porotto et al. 2010).

The effectiveness of fusion inhibitor peptides relies on the strength of the interaction between the peptide and the target protein, on the location of the peptide, which must be in close proximity to the target, and on the peptide orientation at the target membrane (Porotto et al. 2010). Cholesterol moieties are able to orientate and localize the peptides on the target membrane, leading to an strategy that improve pharmacokinetic properties (Lee et al. 2011).

The major challenge in developing fusion inhibitors for influenza virus has been the fact that this virus fusion occurs at intracellular locations. One strategy that has been applied is to tag the peptide with a lipid moiety. Lipid-tagged peptides may follow the membrane attached HA from the cell surface to the site of fusion activation (Lee et al. 2011).

The peptides used in this Thesis were designed based on HA_2 and, in order to overcome the intracellular fusion problem, they were tagged with cholesterol. These peptides are supposed to inhibit the fusion of influenza by trapping the HA in a transient conformation. Studies with Influenza-PEG_4-Chol peptide showed that it is possible to prevent the progression of fusion (Lee et al. 2011).

1.7 Objectives in the context of the state-of-art

At low pH, the hemagglutinin of influenza virus undergoes an irreversible conformational change that potentiates its essential membrane fusion function. Inhibiting this conformational change has been the key for the development of new fusion inhibitor peptides against all the virus containing hemagglutinin in their composition and had a similar fusion process, in order to develop a broad-spectrum anti-fusion peptide.

Influenza-PEG_4-Chol was already studied against live viruses. It was found that this peptide was able to trap HA in a transient intermediate state after fusion triggering and before completion of the refolding steps that drive the merging of the membranes (Lee et al. 2011). Therefore, Influenza-Untagged and (Influenza-PEG_4)$_2$-Chol were derived from this peptide, in order to evaluate the activity of the peptide without a lipid moiety or with two peptide chains, respectively.

Information obtained on previous studies at Nuno Santos Lab, Biomembrane Unit, at IMM, Lisbon, Portugal, with fusion inhibitor peptides against HIV, such as enfuvirtide (Matos, Castanho, et al. 2010), C34, C34-Chol (Augusto et al. 2014), sifuvirtide (Matos, Freitas, et al. 2010) and T-1249 (Matos, Castanho, et al. 2010), shows that their interaction with membranes was a significant point to characterize and understand the mechanism of action of these peptides. Therefore, for the fusion inhibitor peptides against influenza virus, the same principle was applied. The aim of this thesis was to study the interaction between Influenza-Untagged, Influenza-PEG_4-Chol and (Influenza-PEG_4)$_2$-Chol with biomembrane model systems and human blood cells.

Fluorescence spectroscopy methodologies were used to characterize this interaction. These methods were used to assess the partition coefficient of the peptides with POPC and POPC:Chol (2:1) vesicles, and the peptide aggregation, by the ANS probe. Quenching studies with acrylamide (aqueous quencher) and with 5NS and 16NS (lipophilic quenchers) were performed to evaluate the in-depth location of the Trp residues at the membrane. Since the direct measure of the peptide intrinsic tryptophan fluorescence is useless in cells, the fluorescent lipophilic probe di-8-ANEPPS was used as an indirect reporter to evaluate the interactions between the peptides and human blood cells (erythrocytes and lymphocytes).

2 Materials and Methods

2.1 Materials

2.1.1 Peptides

The peptides tested during the experiments for this thesis (Figure 11) were synthesized from the HA_2 chain of hemagglutinin, which is the most conserved chain. Influenza-Untagged (Mw=4265.5 g/mol), Influenza-PEG_4-Chol (Mw=4882.5 g/mol) and (Influenza-PEG_4)$_2$-Chol (Mw=9755.8 g/mol) peptides were obtained on the context of a collaboration project with Dr. Matteo Porotto and Prof. Anne Moscona (Departments of Pediatrics, Microbiology & Immunology, and Physiology & Cellular Biophysics at Columbia University Medical Center, New York, USA). Stock solutions of each peptide were prepared in dimethylsulfoxide (DMSO), with a final concentration of 500 µM, and stored at -20°C.

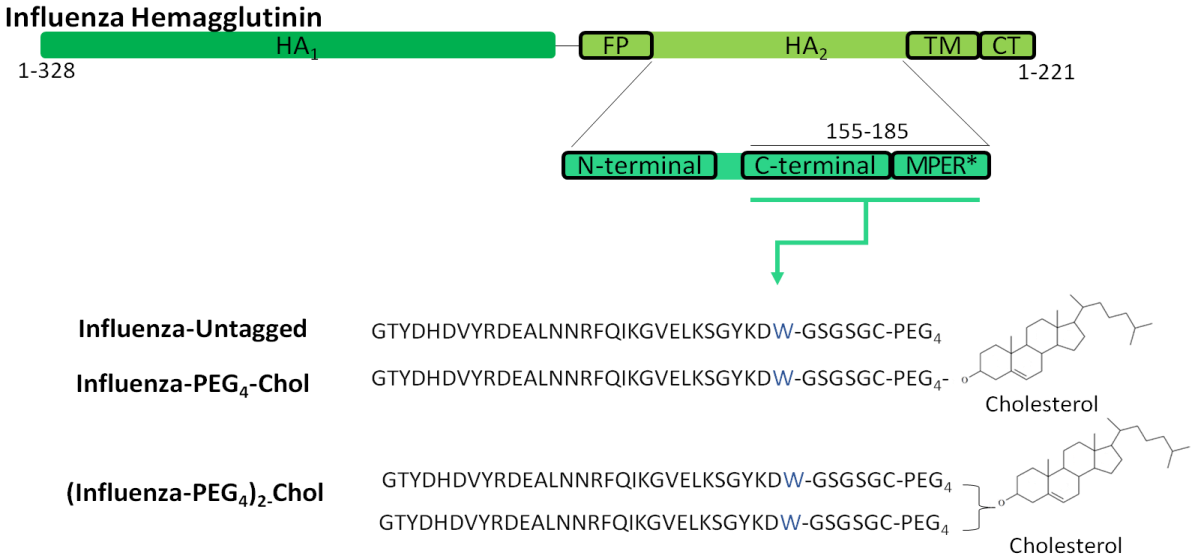

Figure 11: Flu peptides sequence
In this figure are represented the three principal components: amino acid residues sequence, polyethylene glycol (PEG) spacer and cholesterol moiety. The tryptophan residues are highlighted by blue

2.1.2 Biological Material

Human blood samples were obtained from healthy volunteer donors, with their previous written informed consent, at Instituto Português do Sangue (IPS), Lisbon. Samples were collected to K_3EDTA anticoagulant tubes (Vacuette, Greiner Bio-One, Kremsmünster, Austria). This study was approved by the Joint Ethics Committee of Faculdade de Medicina da Universidade de Lisboa and Hospital de Santa Maria (Lisbon).

2.1.3 Other reagents

POPC (1-palmitoyl-2-oleoyl-sn-glycero-3-phosphocoline) was purchased from Avanti Polar Lipids (Alabaster, AL, USA). NaCl, L-tryptophan, DMSO, sodium citrate, chloroform, and acrylamide were from Merk (Darmstadt, Germany). HEPES (4-(2-hydroxyethyl)-1-piperazineethanesufonic acid), cholesterol, Pluronic-F127, ANS (8-anilino-1-naphthalenesulfonic acid), 5NS (5-doxyl-stearic acid) and 16NS (16-doxyl-stearic acid) were acquired from Sigma-Aldrich (St. Louis, MO, USA). The fluorescence probe di-8-ANEPPS (4-[2-[6-(dioctylamino)-2-naphthalenyl]ethenyl]1-(3-sulfopropyl)-pyridinium) was purchased from Invitrogen – Molecular Probes (Eugene, OR, USA). Lymphoprep™ was obtained from Stemcell Technologies (Vancouver, BC, Canada).

The working buffers used throughout the studies were HEPES 10mM pH 7.4 with NaCl 150mM and sodium citrate 10 mM pH 5.0 with NaCl 150mM. L-Tryptophan 500 µM stock solution was prepared in buffer, while ANS 2 mM and acrylamide 2 M were prepared in ultrapure H_2O. Stock solutions of the fluorescence probe di-8-ANEPPS 1 mg/mL and the lipophilic quenchers 5NS and 16NS 70 mM were prepared in ethanol. All stock solutions were stored at 4˚C, except 5NS and 16NS that were stored at -20˚C.

2.2 Methods

2.2.1 Biomembrane (model) systems preparation

2.2.1.1 Liposomes

Different lipids such as POPC and Chol were weighed to generate vesicles of different compositions: pure POPC and POPC:Chol (2:1). To dissolve the phospholipids organic solvents such as chloroform were used and mixed in a round-bottom flask. By drying the solvent out with a gentle N_2 flow, a thin lipid film was formed. To guarantee that solvent residues were eliminated and therefore, obtain a completely dried film, the flask was connected to a vacuum pump overnight (Esbjörner et al. 2007). In order to form a liposome suspension of multilamellar vesicles (MLV), the dried film was hydrated with buffer and then 8 freeze-thaw cycles were performed. Large unilamellar vesicles (LUV) were obtained by extrusion (Mayer et al. 1986) using a mini-extruder (Avanti Polar Lipids, Alabaster, AL, USA), 1001 RN syringes (Hamilton, Reno, NV, USA) and 100 nm pore polycarbonate 10 nm diameter filters (Nucleopore-Whatman, Kent, UK). LUV with, approximately, 100 nm of diameter were obtained and used as model system for biological membranes.

2.2.1.2 Biological Samples

- Erythrocytes isolation

  In order to remove plasma and the buffy-coat (platelets and white blood cells layer between erythrocytes and plasma), the blood sample was centrifuged for 10 min at 1200 *g* (Sorvall TC6 Centrifuge, H400 rotor). Afterwards, isolated erythrocytes were washed three times with working buffer and 100% hematocrit sample was obtained (Matos, Freitas, et al. 2010).

❖ Peripheral blood mononuclear cells (PBMC) isolation

PBMC were isolated by density gradient using Lymphoprep™. The blood samples were centrifuged for 30 min at 400 *g*, allowing the isolation of the buffy-coat containing the wanted cells (Matos, Castanho, et al. 2010). Then, isolated PBMC were washed three times, with working buffer and, in order to prevent contaminations, an erythrocytes lysis buffer (157 mM NH_4Cl, 10 mM $KHCO_3$, EDTA 5%, pH 7.4). In the washing steps, samples were centrifuged for 5 min at 1500 *g*.

2.2.2 Partition coefficient determination

Intrinsic peptide fluorescence deriving from the naturally fluorescent amino acid tryptophan can provide information on conformational changes (Hawe et al. 2008) and it is a valuable tool to quantify their insertion on lipid membranes, such as LUV (Matos, Franquelim, et al. 2010). The influenza peptides in study contain tryptophan residues (1 residue in the case of the Influenza-Untagged and Influenza-PEG_4-Cholesterol and 2 residues for (Influenza-PEG_4)$_2$-Cholesterol). The partition coefficient of a molecule between a lipid and an aqueous phase can be estimated if a difference occurs in a fluorescence parameter of the partitioning molecule or the incorporation of the molecule in the membrane leads to a change on a fluorescence property of a membrane probe.

For each peptide, the partition coefficient can be described as (Matos, Franquelim, et al. 2010; Santos et al. 2003):

$$K_p{}' = \frac{\frac{\eta_{peptide,L}}{\eta_L + \eta_{peptide,L}}}{\frac{\eta_{peptide,W}}{\eta_w + \eta_{peptide,W}}} \qquad (2.1)$$

where η_L and η_W are the moles of the lipid and water and $\eta_{peptide,L}$ and $\eta_{peptide,W}$ are the moles of peptide in lipid and water, respectively. Under most experimental conditions, the quantity of peptide is considerably lower in both phases than the total quantities of water or lipid ($\eta_{peptide,i} << \eta_i$); therefore, this equation can be simplified to:

$$K_p{}' = \frac{\frac{\eta_{peptide,L}}{\eta_L}}{\frac{\eta_{peptide,W}}{\eta_w}} \qquad (2.2)$$

In most of the literature, it is common to represent the partition coefficient as a function of the volumes of each phase (V_i) instead of the water and lipid quantities:

$$K_p = \frac{\frac{\eta_{peptide,L}}{V_L}}{\frac{\eta_{peptide,W}}{V_w}} \quad (2.3)$$

This parameter, named the Nernst partition coefficient, can be related with equation (2.4) by:

$$K_p = K'_p \frac{\gamma_W}{\gamma_L} \quad (2.4)$$

Where $\gamma_i$is the molar volume of water (i =W) or lipid (i =L)

The fluorescence intensity, I, can be measured as long as a peptide fluorescence parameter, such as the quantum yield, has a significant difference between the aqueous environment and the lipid membrane. K_p can be determined measuring the tryptophan fluorescence intensity with a constant peptide concentration and an increasing lipid concentration ([L]). These measurements usually give rise to a hyperbolic I *vs* [L] variation profile that can be fitted using:

$$\frac{I}{I_w} = \frac{1+ K_p\gamma_L\frac{I_L}{I_W}[L]}{1+ K_p\gamma_L[L]} \quad (2.5)$$

POPC and POPC:Chol (2:1) were used to assess the peptides membrane partition coefficient. Successive additions of a 15 mM LUV suspension to a 5 µM peptide solution in HEPES 10 mM in NaCl 150 mM pH 7.4 were done. In case of the partition at pH 5, the working buffer used was sodium citrate 10 mM pH5 in NaCl 150 mM. Preceding the fluorescence emission analysis, an incubation of 10 min was used after each addition of the LUV suspension. The fluorescence emission spectrum of each peptide was recorded between 310 and 450 nm using band widths of 5 and 10 nm, respectively and an excitation wavelength (λ_{exc}) of 280nm was used. The measurements were carried out in a Varian Cary Eclipse Fluorescence Spectrophotometer (Mulgarve, Australia) at room temperature.

2.2.3 Peptide Aggregation

ANS is an environment sensitive probe. It is essentially non fluorescent in water (low quantum yield), becoming fluorescent when bound to hydrophobic sites in proteins (a less polar environment), leading to an increase of the quantum yield and it concomitantly undergoes a blue shift (Veiga et al. 2006). For this reason, this probe is commonly used to evaluate the presence of hydrophobic pockets in proteins and peptides. Since two of the peptides in study have been conjugated with lipid moieties, they may be prone to aggregation in aqueous solution. In order to assess peptide aggregation, the assay was followed by ANS fluorescence emission, with excitation at 369 nm, and the fluorescence emission was collected between 400 and 600 nm using band widths of 5 and 10 nm for excitation and emission, respectively (Henriques et al. 2008). A solution containing 12.8 µM of ANS in HEPES buffer was titrated with a stock solution of the peptide to yield a final peptide concentration in the range of 0–8 µM. Measurements were performed in an Edinburgh Instruments FLS920 Series fluorescence spectrophotometer (Livingston, UK).

2.2.4 Fluorescence Quenching

Quenching is any process that decreases the fluorescence intensity of a given substance. This decrease may be the result of a variety of intermolecular interactions between a fluorophore and a quencher, such as energy transfer, ground-state complex formation, molecular rearrangements, excited-state reactions or collisional quenching (Lakowicz 2006; Valeur & Berberan-Santos 2012).

There are two types of quenching: the collisional or dynamic and the static one. In both cases, molecular contact between the fluorophore and the quencher is required. In the case of the collisional quenching, diffusive encounters between the fluorophore and the quencher occur during the lifetime of the excited state. Upon contact, the fluorophore returns to the ground state, without the emission of a photon (Lakowicz 2006).

Collisional quenching analysis is generally performed by Stern-Volmer plots whereby the fluorescence intensities in the absence and presence of a quencher are collected independently and the ratio between these intensities is plotted as a function of quencher

concentration, from which Stern-Volmer constant is calculated (Geddes & Lakowicz 2009). The Stern-Volmer equation is:

$$\frac{I_0}{I} = 1 + K_{sv}[Q] \quad (2.6)$$

where I_0 and I are the fluorescence intensities in the absence and presence of quencher, respectively, K_{sv} is the Stern-Volmer constant and $[Q]$ the concentration of quencher (Lakowicz 2006). A high K_{sv} would indicate that the fluorophore is efficiently quenched whereas a low K_{sv} would imply the opposite.

Static quenching can occur as a result of the formation of a nonfluorescent ground-state complex between the fluorophore and the quencher (Lakowicz 2006).

This has numerous applications for fluorescence quenching studies, these studies may allow characterization of conformational changes that alter the accessibility of the fluorophore to the quenching agent (Valeur & Berberan-Santos 2012), like we can see in the quenching with acrylamide. In this Thesis, it was also possible to perform quenching analysis to evaluate if the peptides were (or not) buried in the lipid membrane.

2.2.4.1 Quenching by acrylamide

In order to test the accessibility of the peptides tryptophan residues to the aqueous environment acrylamide was used as fluorescence quencher. The emission spectra of 5 µM of influenza peptides incubated (or not) with liposomes and in the presence of acrylamide, whose concentration ranged from 0-60 mM, were measured in 5 mm x 5 mm path length quartz cuvettes (Hellma Analytics, Mulhëim, Germany). The study was done in HEPES buffer and in the presence of POPC 2 mM LUV, by the addition of small volumes of the quencher stock solution. For every addition, at least a 10 min incubation was allowed before the next measurement. In order to promote a selective excitation of tryptophan residues an excitation wavelength of 280 nm was used. The measurements were carried out in a Varian Cary Eclipse Fluorescence Spectrophotometer (Mulgarve, Australia), at room temperature. Data were analyzed by using the Stern-Volmer equation.

2.2.4.2 Quenching by 5NS and 16NS

Fluorescence quenching assays with the lipophilic probes 5NS and 16NS were performed by time-resolved fluorescence spectroscopy, on a LifeSpec II Fluorescence Lifetime Spectrometer (Edinburgh Instruments, Livingston, UK), at room temperature. This is a valuable tool to evaluate the depth of insertion in the membrane. Time-resolved intensity decays were obtained by pulse excitation at 280 nm and fluorescence acquired at 350 nm (20 nm bandwidth) using a 20 ns time span and 1024 channels in a multichannel analyzer.

In these assays, a 5 µM solution of each peptide was incubated with 3 mM POPC LUV. Then, successive additions of small volumes of 5NS or 16NS (in ethanol) were made, keeping the ethanol concentration below 2% (v/v) (Yamazaki et al. 1994). The effective concentration of the quencher at the membrane level was determined from the partition coefficient of both lipophilic molecules to biomembranes (Santos et al. 1998), and ranged from 0 to approximately 0.6 M. For every addition, a 10 min incubation time was allowed before measurement.

The fluorescence lifetime values were obtained from intensity decays fits with a sum of exponentials, using a nonlinear least-squares method based on the Marquardt algorithm (Marquardt 1963). The quality of the fits was evaluated from chi-square (X^2), distributions of the residuals and autocorrelation plots. In order to obtain the depth of the tryptophan insertion in the POPC membrane, the SIMEXDA method (Fernandes, Garcia De La Torre, and Castanho 2002) was applied.

2.2.5 Membrane dipole potential assays by di-8-ANEPPS

The membrane has three types of electrostatic potentials: the surface potential, Ψ_S, generated by the charged head-groups of phospholipids and the ions adsorbed at the interface, resulting in an accumulation of charges in the outer surface of the membrane; the transmembrane potential, $\Delta\Psi$, as a result of an imbalance of charge and an electrical potential difference across the membrane by selective transport of ions, and therefore, a difference in the ion concentration in both sides of the membrane; and the dipole potential, Ψ_d, which arises from the orientation of lipids dipole residues (polar head-groups and

glycerol ester regions) and water molecules hydrating the surface of the membrane (Figure 12) (Matos et al. 2008; Wang 2012; Gross et al. 1994).

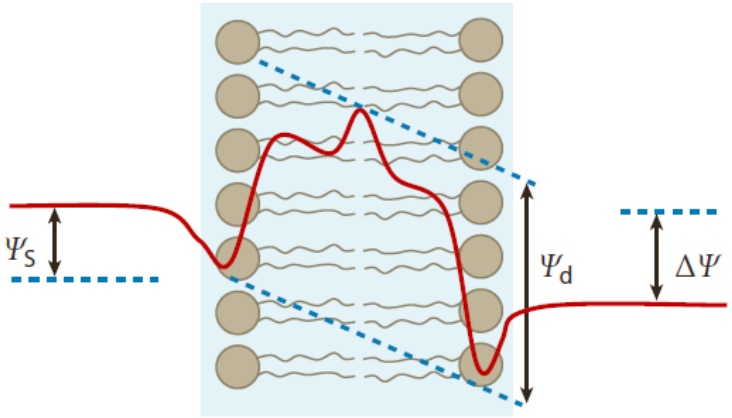

Figure 12: Electrostatic potentials associated with membranes
Ψ_S is the surface potential, $\Delta\Psi$ is the transmembrane potential and Ψ_d is the dipole potential. Adapted from (Wang 2012).

Changes on the dipole potential can reveal interactions at the membrane level. Such alterations may be caused by a destabilization on the lipids organization and/or by the contribution of their own dipoles to the membrane dipole potential, caused by macromolecules interacting with the membrane. The measure of the dipole potential changes is a valuable tool to study the interaction between molecules and the lipid membrane, namely for molecules that are not fluorescent. Furthermore, it is not necessary to derivatize peptides or proteins, which may modify their structure and, consequently, the function and location of these molecules. The influenza fusion inhibitor peptides in study have intrinsic fluorescence but, apart from that, they were chemically modified with a cholesterol moiety to potentially increase their bioavailability at the membrane level. This lipid moiety can interact with the membrane without the involvement of the peptidic region. Since the domain that interacts with the membrane is not fluorescent, to monitor changes on the membrane properties, the use of a membrane potential-sensitive probe, for instance is necessary. In the case of the peptide-cell membrane interaction, this sensitive probe is also a useful reporter (Wang 2012).

Di-8-ANEPPS is the most used probe for measuring dipole potential and allows the monitoring of insertion events, as these tend to change the disposition of the molecular dipoles of membrane phospholipids (Matos et al. 2008).

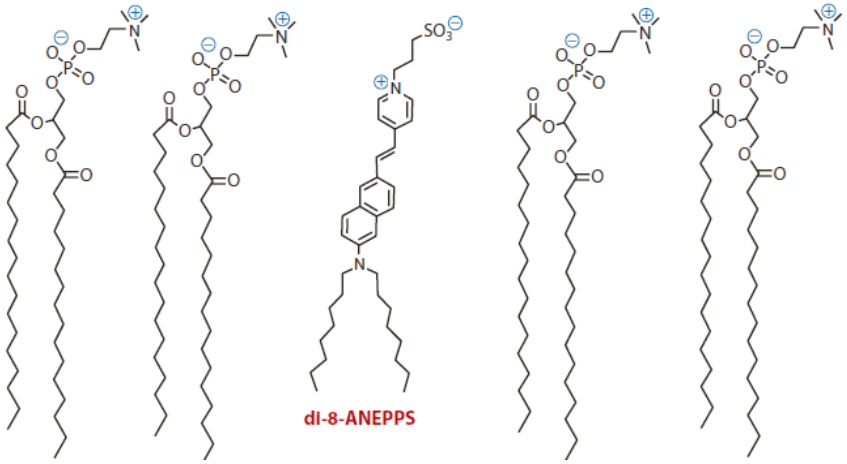

Figure 13: Structure of di-8-ANEPPS between phospholipids
Adapted from (Wang 2012)

This probe has two aliphatic chains (Figure 13), facilitating its incorporation in the outer leaflet of the membrane, attached to a chromophore region that stays near the lipid head-group region and senses the electric fields derived from the dipoles. The changes in the dipole are measured in terms of spectral shifts when the probe is incorporated in the lipid bilayer. A dual wavelength ratiometric measurement can be carried out, with the benefit of the signal being independent of probe or cell concentrations and avoiding photobleaching artifacts. In this Thesis, the work conducted with di-8-ANEPPS was based in the measurement of the excitation spectrum shifts. Excitation wavelengths of 455 and 525 nm were used, with emission set to 670 nm, in order to avoid membrane fluidity artifacts (Clarke & Kane 1997; Gross et al. 1994). The variation of the intensities ratio ($R = I_{455}/I_{525}$) with peptide concentration can be analyzed by a single binding site model (Cladera & O'Shea 1998):

$$\frac{R}{R_0} = 1 + \frac{\frac{R_{\min}}{R_0}[peptide]}{K_d + [peptide]} \qquad (2.7)$$

with the R values normalized for the value in the absence of peptide, R_0. R_{min} is the asymptotic minimum value of R and K_d is the dissociation constant.

Data can be transformed in differential spectra by subtracting the normalized excitation spectra of the probe without the interacting peptide and the spectra in its presence.

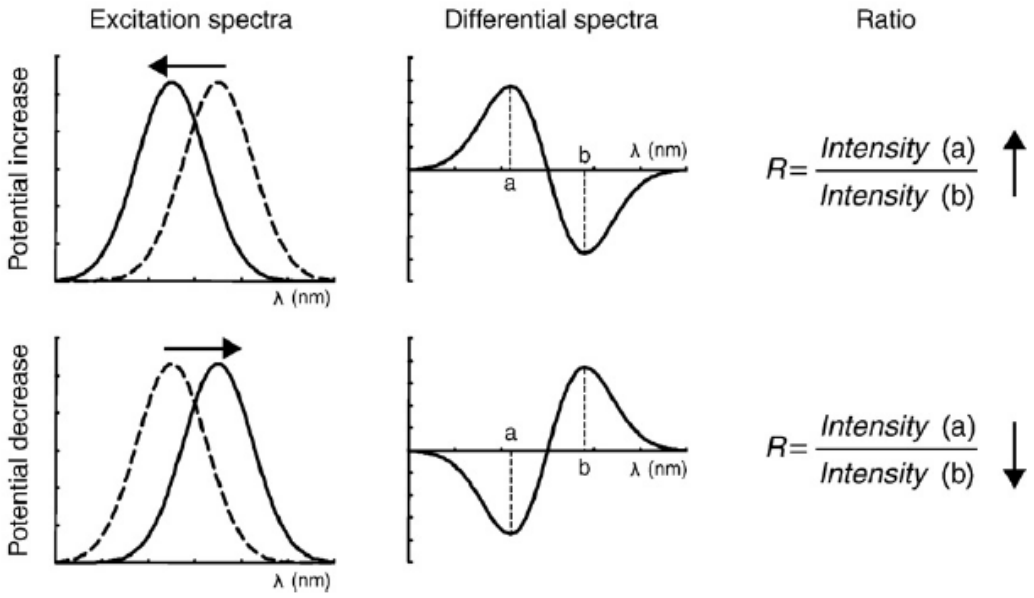

Figure 14: Representation of membrane dipole potential by di-8-ANEPPS
The excitation spectrum shifts in response to changes in the dipole potential. The differential spectra give a support information to visualize these shifts and to determine the wavelengths of maximal variation (Matos, Franquelim, et al. 2010).

An increased membrane dipole potential leads to a blue shift in the excitation spectrum, resulting in an increased ratio value. On the other hand, a decrease in membrane dipole potential leads to a red shift and a consequent decrease on the ratio. If there is no interaction between the peptide and the membrane, the dipole potential remains unchanged and a shift in the excitation spectra is not expected.

2.2.5.1 Membrane dipole potential of LUV

LUVs were labeled with di-8-ANEPPS, in order to assess membrane dipole potential. To maximize the incorporation of the probe in the membrane, a freshly prepared LUV suspension containing 500 µM of lipid was incubated overnight with di-8-ANEPPS. Preceding fluorescence measurements, each peptide, with concentrations raging from 0 to7 µM, was incubated with di-8-ANEPPS-labeled LUV for 1 h at room temperature. An aqueous solution of cholesterol (from a DMSO stock solution) was also incubated in the same conditions as

the peptides, in order to serve as a control. Excitation spectra and the ratio of intensities at the excitation wavelengths of 455 and 525 nm ($R = I_{455}/I_{525}$) were obtained with the emission wavelength set to 670 nm. Excitation and emission slits were set to 5 and 10 nm, respectively.

2.2.5.2 Membrane dipole potential of erythrocytes

From a previously prepared 10% hematocrit sample, a 1% hematocrit suspension of erythrocytes in HEPES buffer supplemented with 0.05% Pluronic F-127 was used for labelling with di-8-ANEPPS 10 µM. The suspension with erythrocytes and di-8-ANEPPS was incubated with gentle agitation, protected from the light, at room temperature, for 1 h. After this time, in order to remove the unbound probe, two wash cycles were performed with centrifugations at 1500 *g* for 5 min. The influenza fusion inhibitor peptides, with a final concentration ranging from 0 to 6 µM, were incubated with the labelled erythrocytes for 1 h at room temperature and then the fluorescence measurements were performed.
The experimental conditions of fluorescence measurements were identical to those previously described for LUV.

2.2.5.3 Membrane dipole potential of PBMC

PBMC were counted in a Moxi Z Mini automated Cell Counter (ORFLO Technologies, Ketchum, ID, USA). A suspension was prepared with a final concentration of 3000 cells/mL in 0.05% Pluronic F-127 supplemented HEPES buffer with di-8-ANEPPS 3.3 mM. The PBMC were incubated with the fluorescent probe suspension at room temperature with gentle agitation and protected from the light. The unbound probe was removed by centrifugations at 1500 *g* for 5 min. The peptides were incubated with PBMC at 100 cells/µL during 1 h, before the fluorescence measurements. The experimental conditions of fluorescence measurements were identical to those previously describe.
To test the membrane dipole potential of erythrocytes and PBMC at pH 5, sodium citrate buffer was used in the finals centrifugations, after the suspension incubation.

3 Results and Discussion

3.1 Partition coefficient determination

Partition into biomembranes is particularly relevant, especially for many molecules that have biological membranes as their target (Santos et al. 2003)

As shown in figure 15 A and B, the peptides tagged with cholesterol had a decrease in the fluorescence intensity in the presence of LUV of POPC and POPC:Chol (2:1) at pH 7.4. In the case of the Influenza-Untagged peptide, no significant changes were observed, demonstrating either an absence of significant peptide-membrane interaction or an interaction in which the tryptophan residues are not involved.

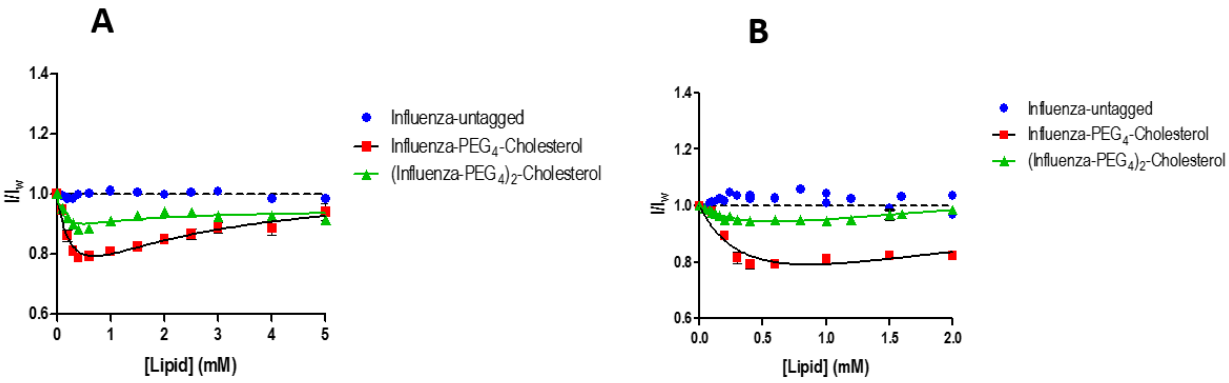

Figure 15: Partition of the peptides to lipid vesicles
Membrane partition with POPC vesicles (A) and POPC:Chol (2:1) vesicles (B), in HEPPES buffer 10mM pH 7.4

In order to mimic the acidic conditions inside the endosome, the partition assays were also performed at pH 5. Figure 16 A and B shows that the (Influenza-PEG_4)$_2$-Chol peptide is the only one that has a significant decrease in fluorescence intensity either in POPC or POPC:Chol vesicles. In this case, not only the untagged peptide but also Influenza-PEG_4-Chol do not seem to interact with the membrane.

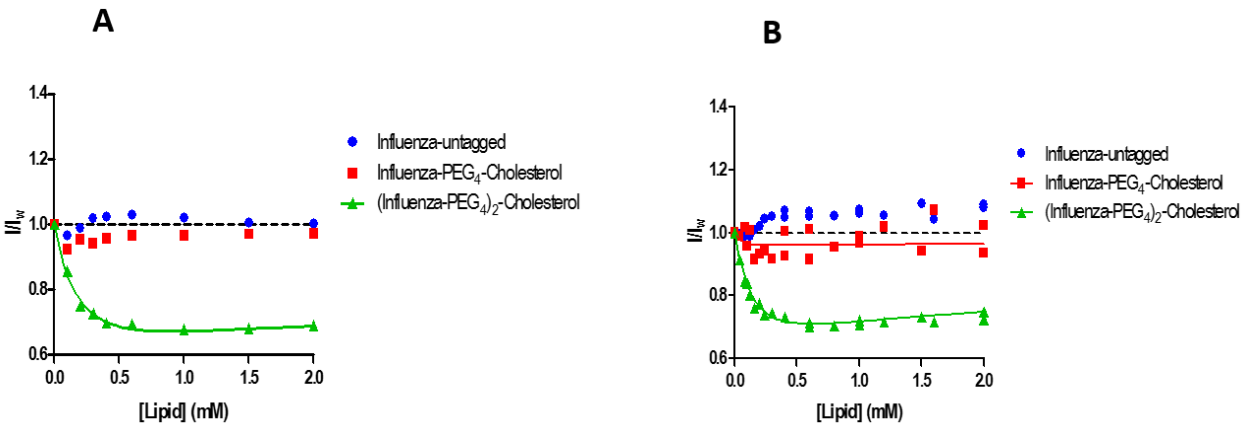

Figure 16: Partition of the peptides to lipid vesicles
Membrane partition with POPC vesicles (A) and POPC:Chol (2:1) vesicles (B), in sodium citrate buffer 10mM pH 5

In order to quantify the extent of interaction of peptides with LUV, the partition coefficient between the lipid and aqueous phases was calculated by fitting with Equation 2.5 (Table 1). In the case of the untagged peptide, no significant peptide-membrane interactions were observed. Previous studies performed for fusion-inhibitory peptides with no lipid moiety or a lipid-binding domain also showed no interaction with lipid (Hollmann et al. 2013). Thus the absence of interaction between the untagged peptide with the lipid membrane is not surprising considering that this peptides primary structure does not include an identifiable lipid-binding domain.

Influenza-PEG_4-Chol seems to have a comparable affinity for POPC and POPC:Chol (2:1), as similar K_p values were obtained at pH 7.4. When tested for acidic pH the peptide did not interact with the membrane composed with either POPC or POPC:Chol (2:1). As mentioned before, the hemagglutinin protein at pH 5 undergoes a conformational rearrangement to expose the fusion peptide to the membrane in order to infect the cell (Russell et al. 2008). This peptide may suffer an alteration in the tridimensional structure, at pH 5, leading to a decrease in the affinity to membranes.

In the case of the (Influenza-PEG_4)$_2$-Chol, it seems to interact with the membrane in all conditions tested, as we can see by looking at the K_p values (Table 1). However, the major interaction appears to occur with POPC:Chol (2:1) vesicles, at pH 5. As seen before for other membrane fusion inhibitor peptides with lipid moieties (Augusto et al. 2014), (Influenza-PEG_4)$_2$-Chol presented more affinity to cholesterol-rich membranes.

Table 1: Partition coefficients of the peptides
In the cases in which, due to the fact that there are no significant changes in fluorescence intensity, it was not possible to fit the equation to calculate the K_p, is considered as approximately 0, and I_L/I_W is represented in the table by (–).

		POPC		POPC:Chol (2:1)	
	pH	**K_p**	**I_L/I_W**	**K_p**	**I_L/I_W**
Influenza-Untagged	7.4	≈ 0	–	≈ 0	–
	5.0	≈ 0	–	≈ 0	–
Influenza-PEG_4-Chol	7.4	2692 ± 310	1.04 ± 0.04	2234 ± 569	1.16 ± 0.33
	5.0	≈ 0	–	≈ 0	–
(Influenza-PEG_4)$_2$-Chol	7.4	4278 ± 1668	0.95 ± 0.02	1667 ± 383	1.15 ± 0.08
	5.0	4287 ± 1236	0.76 ± 0.06	5119 ± 334	0.83 ± 0.01

3.2 Peptide Aggregation - ANS

The peptides conjugated with lipid moieties are prone to self-aggregation when in aqueous solutions (Ward et al. 2013). To evaluate the aggregation of these peptides, we used ANS, which is an amphiphilic fluorescent probe sensitive to its microenvironment and is commonly used to evaluate the presence of hydrophobic pockets in proteins and peptides.

In this case, for Influenza-PEG_4-Chol and (Influenza-PEG_4)$_2$-Chol, it was possible to see an increase in the fluorescence intensity and a significant blue shift of the maximum wavelength of ANS emission (Figure 17), which could indicate the presence of aggregates in solution. This happens because the tryptophan residues are in a less polar environment, leading to a higher quantum yield (Franquelim et al. 2008).

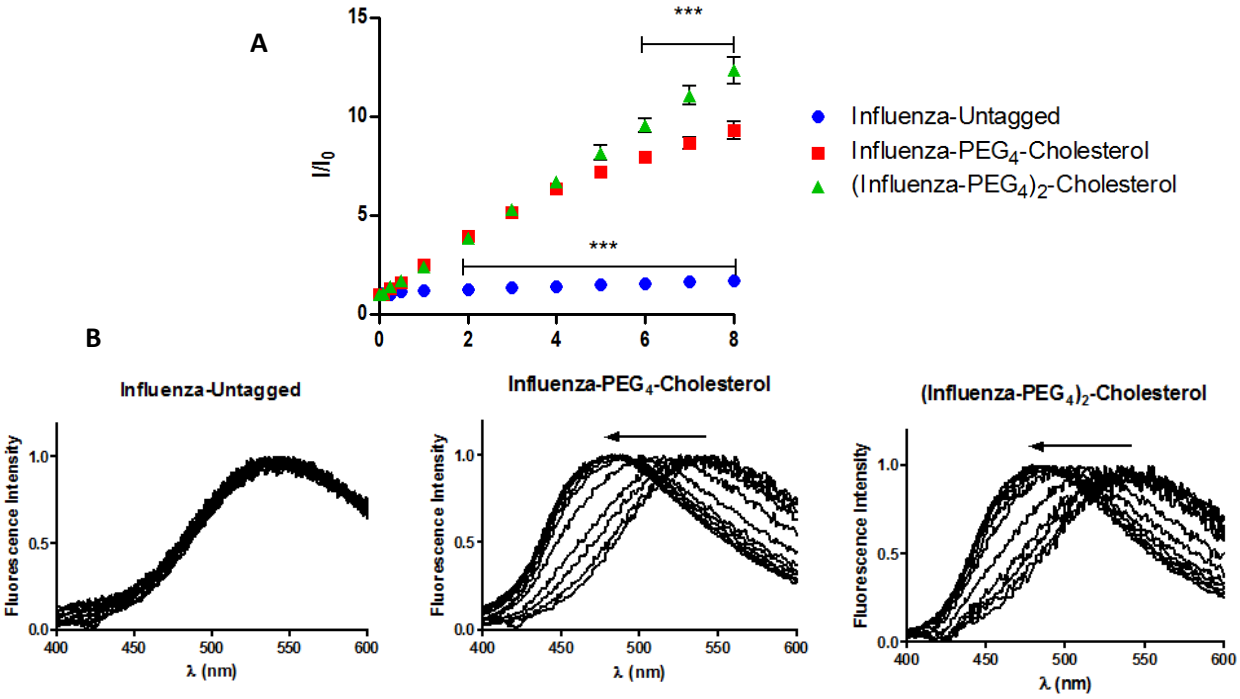

Figure 17: Aggregation of the different peptides: fluorescence properties
(A) Dependence of fluorescence intensity with peptide concentration; (B) Fluorescence spectra that undergo a blue-shift with increasing peptide concentration. ***there are significant differences in the data (P<0,001).

3.3 Quenching with acrylamide

In order to test the accessibility of the tryptophan residues of the peptides to the aqueous environment, we used acrylamide as a quencher due to its low capacity for penetration into lipid bilayers (Franquelim et al. 2008). The fluorescence of the untagged peptide was more efficiently quenched in buffer than in the presence of vesicles of POPC (Figure 18 and Table 2). This might suggest that in the presence of membranes the peptide changes its conformation and the Trp residue becomes less prone to suffer quenching by acrylamide.

It is noticeable that the quenching of the conjugated peptides in buffer is less efficient than for the untagged peptide (Table 2), which may indicate that the tryptophan residues are less exposed to the aqueous environment.

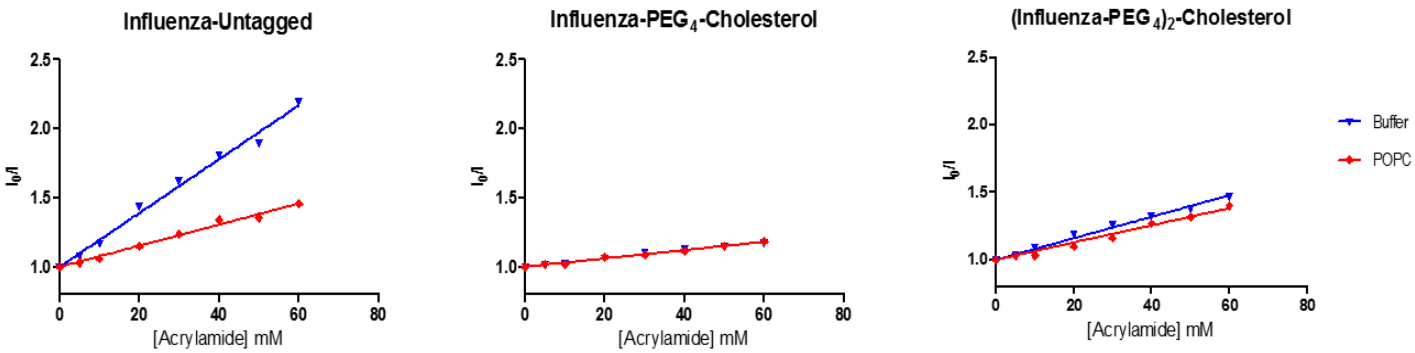

Figure 18: Fluorescence quenching by acrylamide
Quenching in the presence (red) and absence (blue) of POPC vesicles. Continuous lines are fittings of the Stern-Volmer equation

In the case of the peptides with cholesterol, there is no significant difference between the quenching with or without the presence of lipid vesicles. As these peptides exhibits a high tendency to aggregate, the formation those self-assemble structures may be the cause for the absence of differences on the exposure of the tryptophan residues to the aqueous quencher between the peptides present on the aggregates and those interacting with membranes.

Table 2: Stern-Volmer constants obtained for the quenching of the peptides by acrylamide

		Peptides		
System	**Parameters**	**Influenza-Untagged**	**Influenza-PEG_4-Chol**	**(Influenza-PEG_4)$_2$-Chol**
Buffer	K_{sv}	19.49 ± 0.63	3.03 ± 0.16	7.94 ± 0.23
POPC	K_{sv}	7.64 ± 0.19	3.37 ± 0.71	6.36 ± 0.20

3.4 5NS and 16NS Quenching

Accurate determination of the membrane penetration depth is an important step in characterizing membrane interactions of proteins and peptides (Ladokhin 2014).

The in-depth location of the tryptophan residues inserted in lipid membranes was evaluated by using the lipophilic quenchers: 5NS and 16NS. The quencher group (doxyl) of these molecules, present either on the carbon 5 or the carbon 16 of the fatty acyl chain, when inserted in the membrane, has distinct locations: the quencher group of 5NS locates at a

shallower position, whereas 16NS quencher group locates closer to the hydrophobic core, deeply inside the membrane.

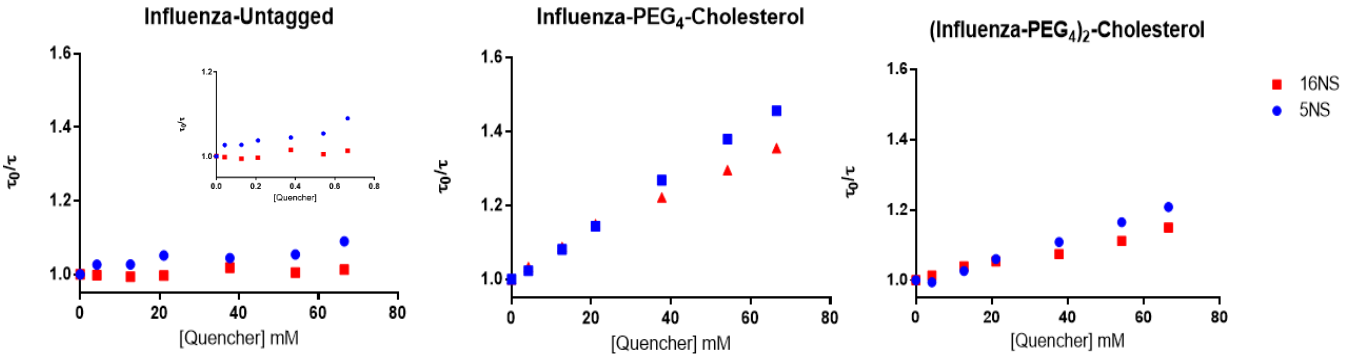

Figure 19: Fluorescence quenching by 5NS and 16NS, determined by time-resolved fluorescence spectroscopy

In general, 5NS and 16NS were able to assess the tryptophan residues in a similar way, suggesting that the tryptophan residues are located in an intermedia position of the membrane (Figure 19).

In order to obtain the in-depth distribution of the fluorophores (Figure 20) the SIMEXDA method was applied. This method takes into account the possibility of static quenching by using a sphere-of-action methodology (Fernandes, Garcia De La Torre, and Castanho 2002).

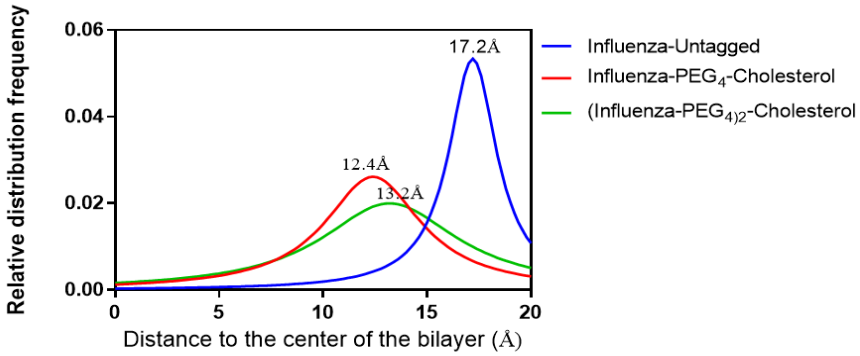

Figure 20: Localization of the peptides inside the membrane of POPC

A relatively shallow position is observed for the peptides analyzed. In average, the Influenza-Untagged is located 17.2 Å away from the center of the bilayer, while Influenza-PEG_4-Chol and the (Influenza-PEG_4)$_2$-Chol were located at 12.4 Å and 13.2 Å, respectively. These results are in agreement with acrylamide quenching data, the Influenza-Untagged is at a shallow

position and, as we can see at quenching with acrylamide, is the one who's tryptophan residue is more accessible to acrylamide and suffers more quenching. In contrast, Influenza-PEG_4-Chol is the peptide with a deepest insertion in the lipid membrane. This comparison should be made, not only looking at the maxima of the distribution (12,4 Å and 13,2 Å), but also at the half-widht at half height (Fernandes et al. 2002). For that reason, it is less exposed to the aqueous environment and suffers less quenching by acrylamide.

The inclusion of the PEG_4 spacer between the peptide region and the cholesterol moiety may contribute to the orientation of the peptide in the membrane, as previously reported (Augusto et al. 2014).

3.5 Membrane Dipole Potential

Peptide-membrane interactions were also evaluated using the lipophilic probe di-8-ANEPPS. As di-8-ANEPPS is an indirect reporter of the membrane dipole potential, any changes caused by the insertion or adsorption of the peptides in/on the membrane can be translated in shifts in the probes excitation spectra.

In the assay with LUV there was a small change in the membrane dipole potential, as we can see in the differential spectra (Figure 19). Only the conjugated were able to interact with the LUV in order to make a small decrease in the membrane dipole potential of the vesicles.

Although in the partition assays the cholesterol-conjugated peptides seemed to have a major interaction with LUVs, it should be pointed that in those assays only the local changes on the tryptophan microenvironment are monitored, whereas the dipole potential changes are able to assess the interaction of the whole fusion inhibitor with the membrane.

In order to quantify the interaction between the peptides and the membranes ratio, R (I_{455}/I_{525}, normalized to the initial value), was plotted as function of the peptide concentration (Figure 21).

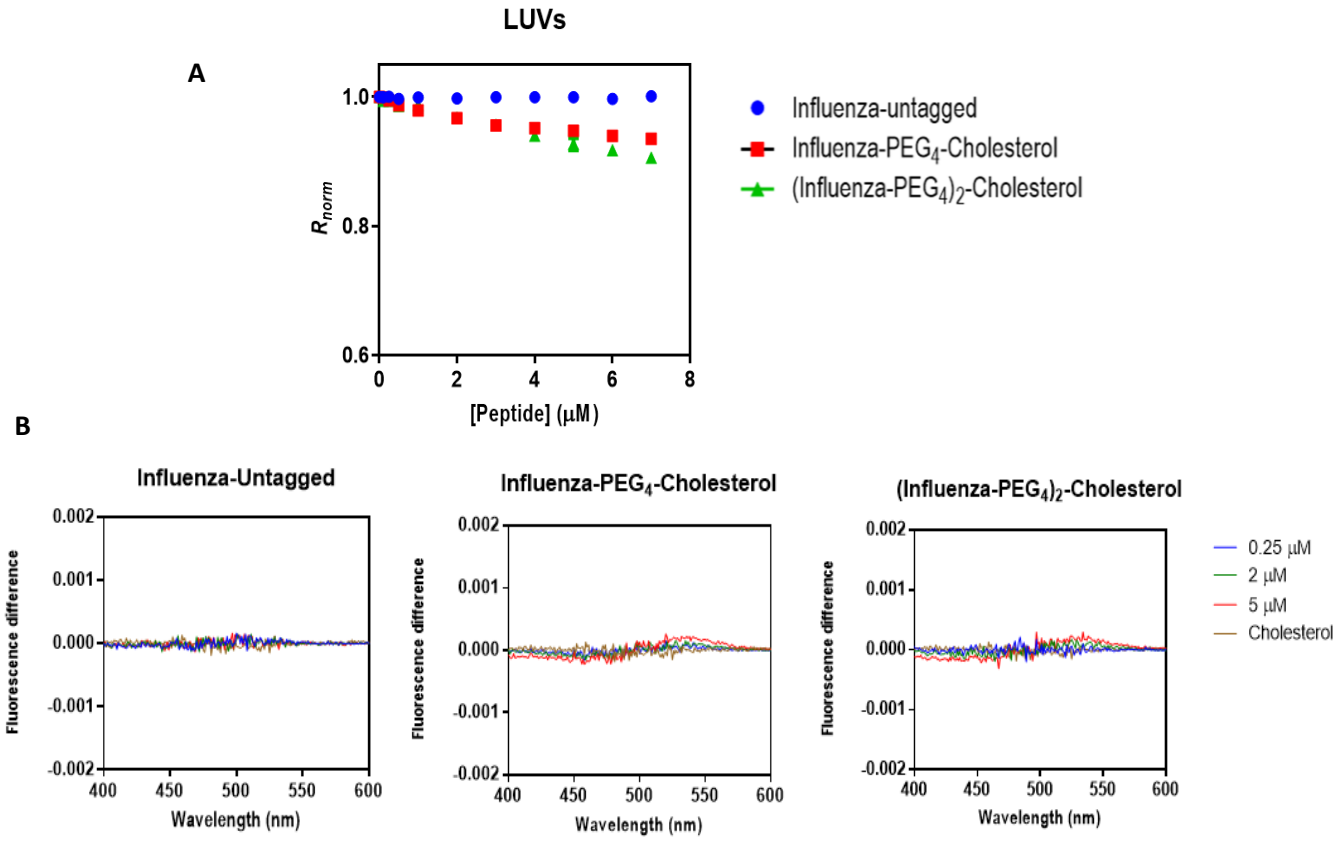

Figure 21: Peptides interactions with di-8-ANEPPS labeled LUV of POPC, at pH 7.4.
(A) Binding profiles of the peptides to LUVs, (B) Differential spectra of di-8-ANEPPS bound to LUV

In order to have a better understanding of what may happen in the bloodstream, we also studied the interaction of these peptides with human blood cells (erythrocytes and PBMC). Data show that the conjugated peptides interact with erythrocytes. There was a decrease of the membrane dipole potential due to the presence of the peptides (Figure 22). In the case of the Influenza-Untagged peptide, there was no interaction until a concentration of 5 µM , however in the last concentration (6 µM) it was possible to observe an alteration in the membrane dipole. Since hemagglutinin is associated with hemagglutination (Mammen et al. 1995), this could be the reason for these decrease of the membrane dipole potential, at a higher concentration of peptide.

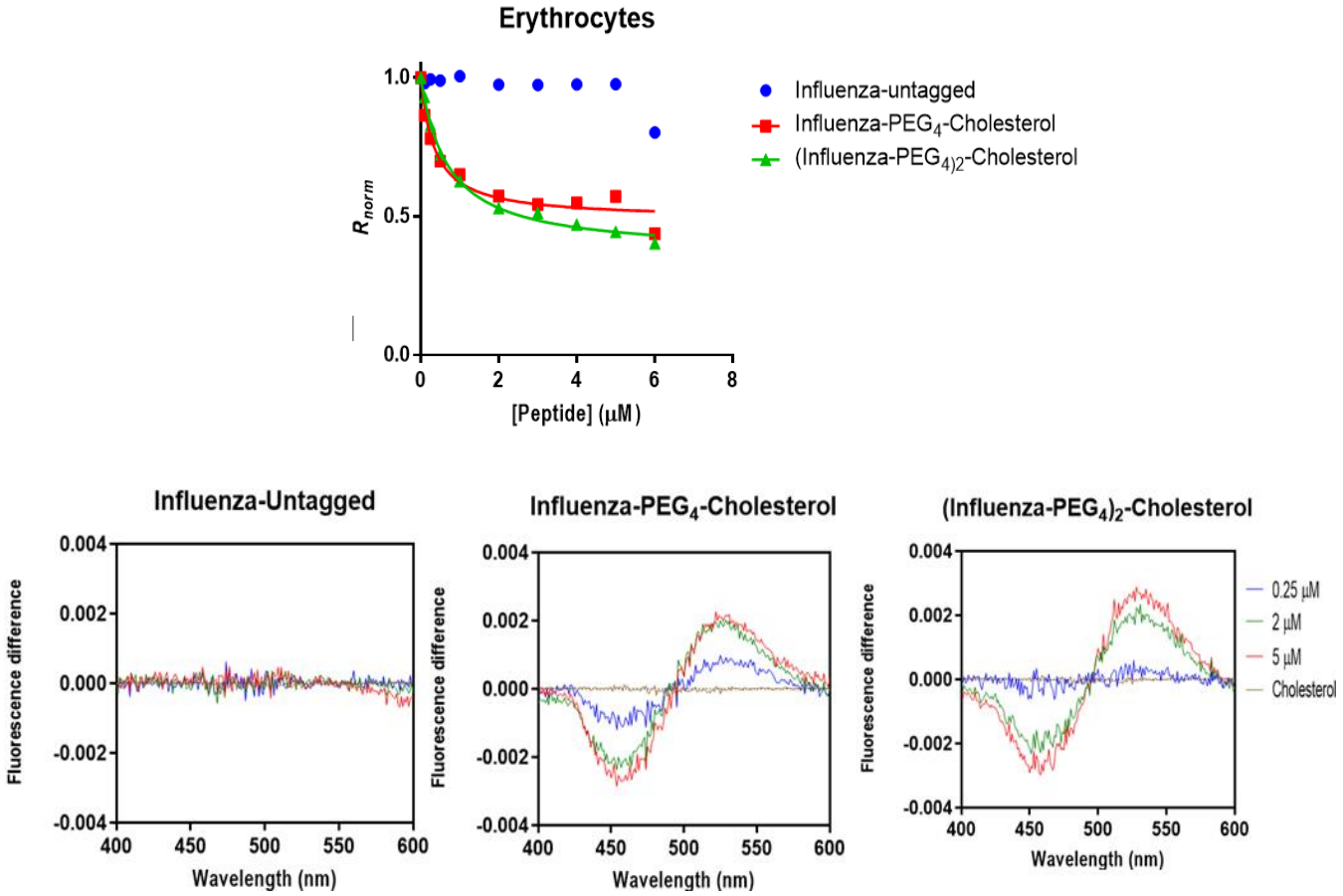

Figure 22: Peptides interactions with di-8-ANEPPS labeled erythrocytes, pH 7.4.
(A) Binding profiles of the peptides to erythrocytes, (B) Differential spectra of di-8-ANEPPS bound to erythrocytes

Similarly, these peptides also interact with PBMCs, as shown in figure 23. In the presence of PBMC, the peptides had almost the same behavior as in the presence of erythrocytes: conjugated peptides are those presenting a major interaction with the membranes and induce a significant decrease in the membrane dipole of PBMC.

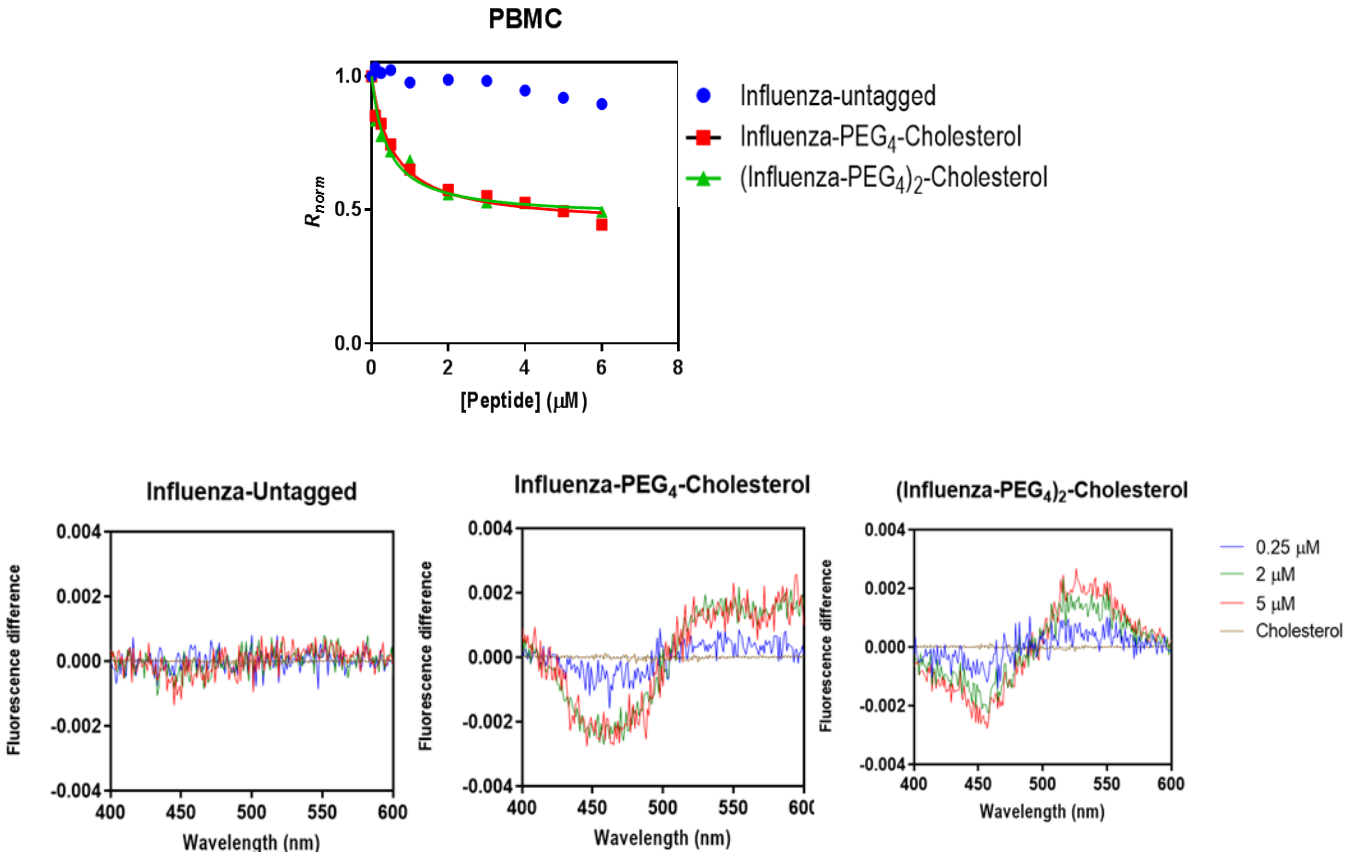

Figure 23: Peptides interactions with di-8-ANEPPS labeled PBMC, at pH 7.4.
(A) Binding profiles of the peptides to PBMC, (B) Differential spectra of di-8-ANEPPS bound to PBMC

To assess the behavior of these peptides when they are in an environment with an acidic pH, as the case of endosomes, where Influenza is known to fuse, the tracking of changes in the membrane dipole potential of blood cell membranes was also performed at these conditions. As we can see in figure 24, at pH 5, the conjugated peptides interact both with erythrocytes and PBMC. On the contrary, to what we saw for erythrocytes at neutral pH, where the untagged peptide seemed to induce hemagglutination, at pH 5 this peptide does not have the same behavior. Previously, it was reported that the hemagglutination only occur in the pH range of 7-10 (Maeda & Ohnishi 1980). This furthers supports our hypothesis of the alteration observed at pH 7.4 being due to hemagglutination.

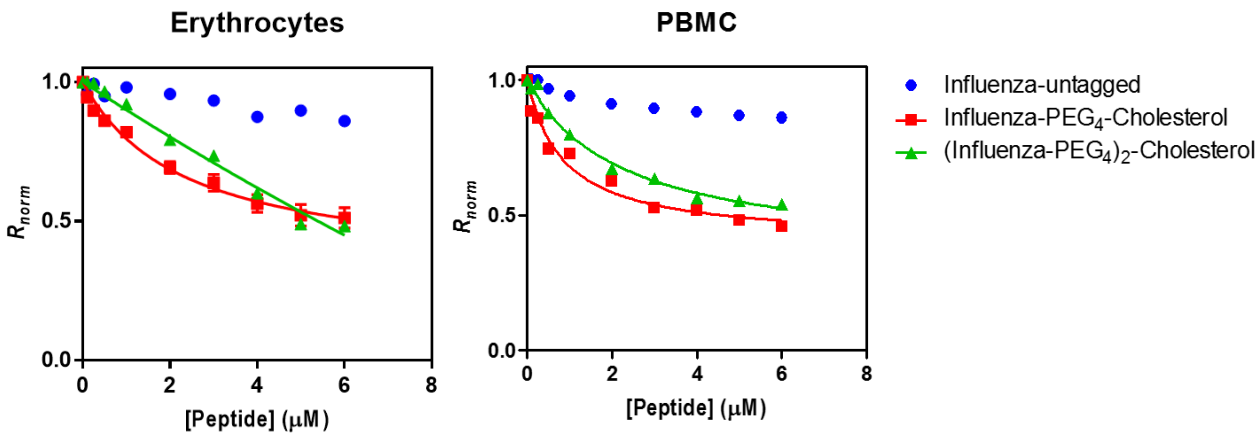

Figure 24: Peptides interactions with di-8-ANEPPS labeled erythrocytes and PBMC, at pH 5.

Apparent dissociation constants were determined by fitting the experimental data of the conjugated peptides with the equation 2.7 (Table 3). The unconjugated peptide data could not be fitted, due to the almost total absence variation of the ratio R as a function of peptide concentration. This should be due to a considerably lower interaction of the peptide with the blood cells membranes, regardless of the pH value tested, when compared with the conjugated molecules, in agreement with the partition data.

Influeza-PEG_4-Chol has a higher affinity (lower K_d) to erythrocytes membranes at neutral pH, while (Influenza-PEG_4)$_2$-Chol has a higher affinity to PBMC membranes at the same pH. In acidic environment, their affinity to blood cells membranes decrease (increased K_d). Only Influenza-PEG_4-Chol presents just a slight decrease on affinity for PBMC membrane at pH 5. As previously reported HIVP4, HIV fusion inhibitor peptide, also has higher affinity towards PBMC membrane, with the peculiarity of being also a dimer (Augusto et al. 2014).

As common for mammalian cells, erythrocytes and PBMC have cholesterol in their membrane composition (Almizraq et al. 2013; Leidl et al. 2008). These cholesterol-conjugated peptides seem to have a higher affinity with these cells membrane than with the POPC vesicles. This reinforces that the peptides may interact preferentially with cholesterol containing membranes.

Table 3: Apparent dissociation constants and R_{min} values of the peptides for erythrocytes and PBMC, at different pH values, calculated fitting the experimental data with equation 2.7

		Erythrocytes		PBMC	
	pH	**K_d**	**R_{min}**	**K_d**	**R_{min}**
Influenza-Untagged	**7.4**	-	-	-	-
	5	-	-	-	-
Influenza-PEG_4-Chol	**7.4**	0.29 ± 0.05	-0.48 ± 0.02	0.56 ± 0.06	-0.56 ± 0.01
	5	2.33 ± 0.45	-0.68 ± 0.05	0.86 ± 0,15	-0.60 ± 0.03
(Influenza-PEG_4)$_2$-Chol	**7.4**	0.65 ± 0.13	-0.62 ± 0.03	0.41 ± 0.13	-0.53 ± 0.03
	5	51.34 ± 138	-5.26 ± 12.9	2.23 ± 0.63	-0.65 ± 0.07

4 Conclusions

In the last few years, the need to overcome resistance has greatly fueled the search for new anti-influenza drugs. The targeting of cellular factors involved in the influenza virus replication has received much attention because such an antiviral approach could reduce viral drug resistance (Loregian et al. 2014).

The interaction between peptides with lipid membranes is considered relevant for their mode of action, once the inhibition process occurs in extreme confinement between the cellular plasmatic membrane and the viral envelope (Franquelim et al. 2008). The cholesterol-conjugated peptides can interact with the POPC and POPC:Chol membranes.

By being conjugated with lipid moieties, the peptides are prone to self-aggregation when in aqueous solutions, and as we can see with the ANS assay, the cholesterol-tagged peptides aggregate more than the untagged peptide.

The results of the tryptophan residue position showed that the conjugated peptides are buried in the membrane and therefore, less exposed to aqueous environment. This explain the reason why these peptides suffer less quenching by acrylamide. On the other hand, the unconjugated peptide is at a shallow position in the membrane or interacts only with the membrane surface, being the tryptophan residue highly exposed to acrylamide.

In this Thesis, the peptides that have a lipid moiety showed that they are able to interact with the membrane of the blood cells in order to alter its dipole potential, as expected. At pH 7.4, Influenza-PEG_4-Chol presented the highest affinity to erythrocytes membranes and (Influenza-PEG_4)$_2$-Chol showed the highest affinity to PBMC membranes. However, the same was not seen in the assays with acidic pH. The conjugated peptides had higher K_d values in these conditions, indicating an affinity decrease with the membranes. At lower pH, the deformability of erythrocytes decrease, which indicates that the elastic properties of the membrane could be affected by the pH (Kuzman et al. 2000). If the membrane properties of the erythrocytes suffer alterations in acidic pH, this could be one of the reasons why these peptides had difficulty to interact with it. Peptide binding to blood cells is essential since these peptide drugs are expected to circulate in the bloodstream. When administrated, the fusion inhibitor peptide can be dissolved into the plasma, bound to the plasma proteins and also bound to cell membranes (Matos, Franquelim, et al. 2010).

From all the assays performed, the conjugated peptides had more activity than the unconjugated one. From previous studies, it is known that the majority of the lipid

conjugated viral fusion inhibitors have increased potency when compared to unconjugated ones (Avadisian & Gunning 2013).

It has been suggested that the cholesterol conjugation can be useful for viruses that fuse in endosomes, by endowing the peptides with the ability to be transfected along with the virus to intracellular sites of membrane fusion (Lee et al. 2011). For the conjugated peptides, after being able to be included along the virus in the endosome, bound to the outer leaflet of the cell membrane (which later becomes the inner leaflet of the endosome membrane), their pH-dependent membrane interaction may be an additional advantage. Our membrane potential variation data show that the membrane affinity of these molecules decreases upon changing from pH 7.4 to pH 5.0. Based on this finding, one may propose that after endocytosis, upon the progressive acidification of the endosome, the conjugated peptides will progressively be released from the membrane, becoming confined on the volume of the endocytic pool. This release of the fusion inhibitor will occur together with the (also) pH-driven acquiring by hemagglutinin of its fusogenic and fusion inhibitor-targetable extended conformation. Therefore, the peptides progressively released from the membrane would be able to bind the complementary heptad repeat domain of hemagglutinin, blocking viral fusion and the entry of the viral content into the cytosol, therefore preventing the infection of a target cell.

The Influenza-PEG_4-Chol peptide was already tested with live virus. It is believed that this molecule is able to prevent fusion by blocking the second critical conformation change that drives the membranes together (Lee et al. 2011).

The (Influenza-PEG_4)$_2$-Chol peptide showed to have a better membrane affinity as indicated in some assays, namely partition data and interaction with PBMC. This is in agreement with previous studies where it was reported that dimerization leads to a higher potency and activity (Pessi et al. 2012). That study also suggested that dimerization of CHR-derived peptide, in conjunction with cholesterol tagging, may be a general strategy for increasing its antiviral potency *in vitro*, and that dimers can be effective *in vivo*.

In conclusion, there are three principal components that could improve the antiviral peptide activity and potency, the addition of a PEG spacer that enhance their availability (Augusto et al. 2014); the cholesterol-conjugation that helps to stabilize the peptide in the membrane and increase their half-lives (Johannessen et al. 2011); and dimerization that, as discussed

above, also increase the peptide affinity by increasing the quantity of peptide availability in the membrane (Pessi et al. 2012). Additionally, as explain above, a pH-sensitive membrane interaction may be an advantage for viral fusion inhibitors against viruses which entry occurs through an endocytic pathway (such as influenza). In order to design new antiviral peptides, this information may be needed to take in account.

5 References

Almizraq, R. et al., 2013. Storage of red blood cells affects membrane composition, microvesiculation, and in vitro quality. *Transfusion*, 53(10), pp.2258–2267.

Augusto, M.T. et al., 2014. Improvement of HIV fusion inhibitor C34 efficacy by membrane anchoring and enhanced exposure infection. *Journal of Antimicrobial Chemotherapy*, 69(5), pp.1286–1297.

Avadisian, M. & Gunning, P.T., 2013. Extolling the benefits of molecular therapeutic lipidation. *Mol. Biosys.*, 9(9), pp.2179–88.

Bouvier, N.M. & Palese, P., 2008. The biology of influenza viruses. *Vaccine*, 26(SUPPL. 4), pp.49–53.

Cladera, J. & O'Shea, P., 1998. Intramembrane molecular dipoles affect the membrane insertion and folding of a model amphiphilic peptide. *Biophysical journal*, 74(5), pp.2434–2442.

Clarke, R.J. & Kane, D.J., 1997. Optical detection of membrane dipole potential: Avoidance of fluidity and dye-induced effects. *Biochimica et Biophysica Acta - Biomembranes*, 1323(2), pp.223–239.

Cowling, B.J. et al., 2013. Aerosol transmission is an important mode of infleunza A virus spread. *Nature Communications*, 4, pp.1–11.

Das, K. et al., 2010. Structures of influenza A proteins and insights into antiviral drug targets. *Nature structural & molecular biology*, 17(5), pp.530–8.

Edinger, T.O., Pohl, M.O. & Stertz, S., 2014. Entry of influenza A virus: Host factors and antiviral targets. *Journal of General Virology*, 95(PART 2), pp.263–277.

Esbjörner, E.K. et al., 2007. Membrane binding of pH-sensitive influenza fusion peptides. Positioning, configuration, and induced leakage in a lipid vesicle model. *Biochemistry*, 46(47), pp.13490–13504.

European Centre for Disease Prevention and Control: http://ecdc.europa.eu/en/data-tools/Pages/home.aspx: Last accessed in May 2016

Fernandes, M.X., Garcia De La Torre, J. & Castanho, M.A.R.B., 2002. Joint determination by Brownian dynamics and fluorescence quenching of the in-depth location profile of biomolecules in membranes. *Analytical Biochemistry*, 307(1), pp.1–12.

Fox, A. et al., 2015. Hemagglutination inhibiting antibodies and protection against seasonal and pandemic influenza infection. *Journal of Infection*, 70(2), pp.187–196.

Franquelim, H.G. et al., 2008. Sifuvirtide screens rigid membrane surfaces. Establishment of a correlation between efficacy and membrane domain selectivity among HIV fusion inhibitor peptides. *Journal of the American Chemical Society*, 130(19), pp.6215–6223.

Gatherer, D., 2009. The 2009 H1N1 influenza outbreak in its historical context. *Journal of Clinical Virology*, 45(3), pp.174–178.

Geddes, C.D. & Lakowicz, J.R., 2009. *Reviews in Fluorescence 2007*, New York, NY: Springer New York.

Gross, E., Bedlack, R.S. & Loew, L.M., 1994. Dual-wavelength ratiometric fluorescence measurement of the membrane dipole potential. *Biophysical journal*, 67(1), pp.208–216.

Hamilton, B.S., Whittaker, G.R. & Daniel, S., 2012. Influenza virus-mediated membrane fusion: Determinants of hemagglutinin fusogenic activity and experimental approaches for assessing virus fusion. *Viruses*, 4(7), pp.1144–1168.

Heikkinen, T., 2016. Respiratory viruses and children. *Journal of Infection*, pp.1 – 5.

Henriques, S.T. et al., 2008. PrP(106-126) does not interact with membranes under physiological conditions. *Biophysical journal*, 95(4), pp.1877–1889.

Herfst, S. et al., 2012. Airborne transmission of influenza A/H5N1 virus between ferrets. *Science*, 336(6088), pp.1534–1541.

Hollmann, A. et al., 2013. Conjugation of Cholesterol to HIV-1 Fusion Inhibitor C34 Increases Peptide-Membrane Interactions Potentiating Its Action. *PLoS ONE*, 8(4).

Johannessen, L. et al., 2011. Peptide Structure Stabilization by Membrane Anchoring and its General Applicability to the Development of Potent Cell-Permeable Inhibitors.

ChemBioChem, 12(6), pp.914–921.

Killingley, B. & Nguyen-Van-Tam, J., 2013. Routes of influenza transmission. *Influenza and other Respiratory Viruses*, 7(SUPPL.2), pp.42–51.

Krammer, F. & Palese, P., 2015. Advances in the development of influenza virus vaccines. *Nature reviews. Drug discovery*, 14(3), pp.167–82.

Kuzman, D. et al., 2000. Effect of pH on red blood cell deformability. *Pflügers Archiv*, pp.193–194.

Ladokhin, A.S., 2014. Measuring membrane penetration with depth-dependent fluorescence quenching: Distribution analysis is coming of age. *Biochimica et Biophysica Acta - Biomembranes*, 1838(9), pp.2289–2295.

Lakdawala, S.S. & Subbarao, K., 2012. The Ongoing Battle Against Influenza: The challenge of flu transmission. *Nature Medicine*, 18(10), pp.1468–1470.

Lakowicz, J.R., 2006. *Principles of Fluorescence Spectroscopy.* 3ed., Boston, MA: Springer US.

Lee, K.K. et al., 2011. Capturing a fusion intermediate of influenza hemagglutinin with a cholesterol-conjugated peptide, a new antiviral strategy for influenza virus. *Journal of Biological Chemistry*, 286(49), pp.42141–42149.

Leidl, K. et al., 2008. Mass spectrometric analysis of lipid species of human circulating blood cells. *Biochimica et Biophysica Acta - Molecular and Cell Biology of Lipids*, 1781(10), pp.655–664.

Loregian, A. et al., 2014. Antiviral strategies against influenza virus: towards new therapeutic approaches. *Cellular and molecular life sciences*, 71(19), pp.3659–3683.

Maeda, T. & Ohnishi, S., 1980. Activation of inluenza virus by acidic media causes hemolysis and fusion of erythrocytes. *FEBS letters*, 122(2).

Mammen, M., Dahmann, G. & Whitesides, G.M., 1995. Effective inhibitors of hemagglutination by influenza virus synthesized from polymers having active ester groups. Insight into mechanism of inhibition. *Journal of medicinal chemistry*, 38(21), pp.4179–4190.

Marquardt, D.W., 1963. An Algorithm for Least-Squares Estimation of Nonlinear Parameters. *Journal of the Society for Industrial and Applied Mathematics*, 11(2), pp.431–441.

Matos, P.M., Franquelim, H.G., et al., 2010. Quantitative assessment of peptide-lipid interactions. Ubiquitous fluorescence methodologies. *Biochimica et Biophysica Acta - Biomembranes*, 1798(11), pp.1999–2012.

Matos, P.M., Freitas, T., et al., 2010. The role of blood cell membrane lipids on the mode of action of HIV-1 fusion inhibitor sifuvirtide. *Biochemical and Biophysical Research Communications*, 403(3-4), pp.270–274.

Matos, P.M., Castanho, M.A.R.B. & Santos, N.C., 2010. HIV-1 fusion inhibitor peptides enfuvirtide and T-1249 interact with erythrocyte and lymphocyte membranes. *PLoS ONE*, 5(3), pp.1–8.

Matos, P.M., Gonçalves, S. & Santos, N.C., 2008. Interaction of peptides with biomembranes assessed by potential-sentitive fluorescent probes. *Journal of peptide science : an official publication of the European Peptide Society*, 14(10), pp.407–415.

Mayer, L.D., Hope, M.J. & Cullis, P.R., 1986. Vesicles of variable sizes produced by a rapid extrusion procedure. *BBA - Biomembranes*, 858(1), pp.161–168.

Medina, R. a & García-Sastre, A., 2011. Influenza A viruses: new research developments. *Nature reviews. Microbiology*, 9(8), pp.590–603.

National Institute of Allergy and Infectious Disease: https://www.niaid.nih.gov: Last accessed in May 2016

Neumann, G., Noda, T. & Kawaoka, Y., 2009. Emergence and pandemic potential of swine-origin H1N1 influenza virus. *Nature*, 459(7249), pp.931–9.

Pessi, A. et al., 2012. A general strategy to endow natural fusion-protein-derived peptides with potent antiviral activity. *PLoS ONE*, 7(5), pp.1–9.

Plemper, R.K., 2011. Cell entry of enveloped viruses. *Current Opinion in Virology*, 1(2), pp.92–100.

Porotto, M. et al., 2010. Viral entry inhibitors targeted to the membrane site of action. *Journal of virology*, 84(13), pp.6760–8.

Practical Applications of Immunology: http://classes.midlandstech.edu: Last accessed in May 2016

Roberts, P.C., Garten, W. & Klenk, H.D., 1993. Role of conserved glycosylation sites in maturation and transport of influenza A virus hemagglutinin. *Journal of virology*, 67(6), pp.3048–60.

Russell, R.J. et al., 2008. Structure of influenza hemagglutinin in complex with an inhibitor of membrane fusion. *Proceedings of the National Academy of Sciences of the United States of America*, 105(46), pp.17736–41.

Santos, N.C., Prieto, M. & Castanho, M.A.R.B., 1998. Interaction of the major epitope region of HIV protein gp41 with membrane model systems. A fluorescence spectroscopy study. *Biochemistry*, 37(24), pp.8674–8682.

Santos, N.C., Prieto, M. & Castanho, M.A.R.B., 2003. Quantifying molecular partition into model systems of biomembranes: An emphasis on optical spectroscopic methods. *Biochimica et Biophysica Acta - Biomembranes*, 1612(2), pp.123–135.

Sieczkarski, S.B. & Whittaker, G.R., 2002. Influenza Virus Can Enter and Infect Cells in the Absence of Clathrin-Mediated Endocytosis Influenza Virus Can Enter and Infect Cells in the Absence of Clathrin-Mediated Endocytosis. *Journal of virology*, 76(20), pp.10455–10464.

Skalickova, S. et al., 2015. Perspective of use of antiviral peptides against influenza virus. *Viruses*, 7(10), pp.5428–5442.

Skehel, J.J. & Wiley, D.C., 2000. Receptor binding and membrane fusion in virus entry : The Influenza Hemagglutinin. *Structure*.

Taubenberger, J.K., 2006. The origin and virulence of the 1918 “Spanish” influenza virus. *Proceedings of the American Philosophical Society*, 150(1), pp.86–112.

Taubenberger, J.K. & Morens, D.M., 2010. Influenza: the once and future pandemic. *Public health reports (Washington, D.C. : 1974)*, 125 Suppl , pp.16–26.

Valeur, B. & Berberan-Santos, M.N., 2012. *Molecular Fluorescence: Principles and Applications*, Available at: http://arxiv.org/abs/1011.1669.

Vanderlinden, E. & Naesens, L., 2014. Emerging Antiviral Strategies to Interfere with Influenza Virus Entry. *Medicinal Research Reviews*, 34(2), pp.301–339.

Veiga, S. et al., 2006. Why are HIV-1 fusion inhibitors not effective against SARS-CoV? Biophysical evaluation of molecular interactions. *Biochimica et Biophysica Acta - General Subjects*, 1760(1), pp.55–61.

Vigant, F., Santos, N.C. & Lee, B., 2015. Broad-spectrum antivirals against viral fusion. *Nature Reviews Microbiology*, 13(7), pp.426–437.

Wang, L., 2012. Measurements and implications of the membrane dipole potential. *Annu. Rev. Biochem.*, 81, pp.615–635.

Ward, B.P. et al., 2013. Peptide lipidation stabilizes structure to enhance biological function. *Molecular Metabolism*, 2(4), pp.468–479.

Willem, L. et al., 2012. A Nice Day for an Infection? Weather Conditions and Social Contact Patterns Relevant to Influenza Transmission. *PLoS ONE*, 7(11).

Yamazaki, M. et al., 1994. Direct evidence of induction of interdigitated gel structure in large unilamellar vesicles of dipalmitoylphosphatidylcholine by ethanol: studies by excimer method and high-resolution electron cryomicroscopy. *Biophysical journal*, 66(3 Pt 1), pp.729–733.

Yang, J. et al., 2013. Influenza A virus entry inhibitors targeting the hemagglutinin. *Viruses*, 5(1), pp.352–73.